SUBCELLULAR LOCALIZATION AND CHARACTERIZATION OF *ZEA MAYS* 9-LIPOXYGENASE ISOFORMS

A Thesis

by

JORDAN PETER TOLLEY

Submitted to the Office of Graduate and Professional Studies of
Texas A&M University
in partial fulfillment of the requirements for the degree of

MASTER OF SCIENCE

Chair of Committee,	Hisashi Koiwa
Committee Members,	Michael V. Kolomiets
	Keyan Zhu-Salzman
	Kendal Hirschi
Head of Department,	Daniel R. Lineberger

May 2020

Major Subject: Horticulture

ABSTRACT

Lipoxygenases are often rate limiting enzymes in plant oxylipin biosynthesis pathway. While 13-lipoxygenases have been extensively investigated in plants, characterization of plant 9-lipoxygenases are still in its infancy. Through subcellular localization, biochemical, and genetic analysis, this study characterizes the localization of many of the *Zea mays* 9-lipoxygenases and related lipid metabolism enzymes. This work also includes a more in-depth analysis of *Zea mays* LOX6 using Arabidopsis transgenic plants overexpressing ZmLOX6.

Analysis of *Zea mays* 9-LOX genes tagged with GFP fusion proteins is the initial step in understanding the *in vivo* functionality of 9-lipoxygenases. I found that ZmLOX1 and OPR2 localized to the cytosol. Unexpectedly, ZmLOX4, and ZmLOX5 had shown both cytosolic and tonoplast localization. ZmLOX12 localized to an undetermined organelle cell structure.

ZmLOX6 is an unconventional LOX-like protein in maize and is localized to plastid. When overexpressed in Arabidopsis, ZmLOX6 produced a range of C_5 volatiles and caused a variety of phenotypic such as chlorosis, early flowering in the Arabidopsis host plants. ZmLOX6 overexpressing plants (ZmLOX6-OX) induces chlorosis to wild type plants in close proximity, suggesting C_5 volatiles produced via ZmLOX6 are the cause of the chlorosis. The ZmLOX6-OX lines appear to attract aphids indicating C_5 volatiles function in plant-insect interaction.

ACKNOWLEDGEMENTS

I would like to thank my committee chair, Dr. Hisashi Koiwa, for his patience, guidance and support throughout the course of this research. I also want to thank my committee members, Dr. Michael V. Kolomiets, Dr. Keyan Zhu-Salzman and Dr. Kendal Hirschi for their objective critical analysis of the research. I want to thank all my committee for their patience with my argumentative personality.

I'd like to thank my parents and family for their inspiration and encouragement. I appreciate my father's support of the sciences and to always think outside the box, and my mother's tenacity to never give up. Finally, I'd like to thank my wonderful fiancée for her foundational encouragement, extra lab assistance, and unwavering support has been very important.

CONTRIBUTORS AND FUNDING SOURCES

This work was supervised by a thesis committee consisting of Professor Hisashi Koiwa of the Department of Horticultural Sciences/MEPS, Professor Michael V. Kolomiets Department of Plant Pathology and Microbiology/MEPS, Professor Keyan Zhu-Salzman of the Department of Entomology/MEPS, and Professor Kendal Hirschi the Department of Horticultural Sciences/MEPS.

Gas chromatography mass spectrometry analysis in Chapter III was provided by Ph.D student Zach Gorman of the Department of Plant Pathology and Microbiology. Assistance with confocal microscopy, and a myriad of other miscellaneous assistance with experiments, ideas, and conversation with provided by post-doctoral researcher Dr. Yukihiro Nagashima. Advise, and assistance for insect and chlorophyll data was provided by post-doctoral researcher Dr. Jiaxin Li. Future work for RNAseq analysis was provided by visiting scholar Dr. Midori Ultra-centrifugation rotor assistance was provided by Ph.D student Manish Thakran of Dr. John Mullets lab.

This work was supported by grants from the United States National Science Foundation (IOS-0925561 and IOS-0951272) and United States Department of Agriculture National Institute of Food and Agriculture-Agriculture and Food Research Initiative (2015-67013-22816, 2017-67013-26524, and 2016-77013-24730).

NOMENCLATURE

LOX	Lipoxygenase
GLV	Green leaf volatiles
C_5	5-Carbon Volatiles
JA	Jasmonic Acid
PCR	Polymerase chain reaction
SLiCE	Seamless ligation cloning extract
RT	Reverse transcription
qPCR	Quantitative polymerase chain reaction
GFP	Green fluorescent protein
GC/MS	Gas chromatography mass spectrometry
LC-MS/MS	Liquid chromatography tandem mass spectrometry
GUS	β-glucuronidase
Col	Colombia (Arabidopsis ecotype)
Ler	Landsberg erecta (Arabidopsis ecotype)
RDR6	RNA-dependent RNA polymerase
PEG	Polyethene glycol
OPDA	12-oxo-phytodienoic acid
HPOT	Hydroperoxyoctadeca-9,11,15-trienoic acid

TABLE OF CONTENTS

Page

LIST OF FIGURES

Page

CHAPTER I

INTRODUCTION

1.1 Relationship between drought stress and lipid signaling

Drought is one of the largest problems in global agriculture. Droughts in agriculturally important regions creates economic instabilities in developing countries. Insufficient water availability globally promotes decline of arable land that poses serious challenges on global food security. As the global climate change may progressively exacerbate the severity of drought conditions, water security, and crop drought tolerance become more important around the world (Dai 2013). Research on relationship between lipid signaling and drought and other abiotic stress are still in its infancy. Plant abiotic stress response involves a network of proteins, transcription factors, signaling molecules, etc.

Lipids in plant and animal cells not only maintain a level of cell homeostasis by repairing cell membranes and maintain rigidity and structure within the cell (Golldack et al. 2014). During times of stress polyunsaturated fatty acids can mediate cell damage by free radical scavenging (Golldack et al. 2014; Vellosillo et al. 2013; Okazaki and Saito 2014). They also act as stress signaling precursors for oxylipin production. The most well-known association of stress and lipid signaling is the phytohormone JA, and its role in various defense responses (Golldack et al. 2014; Vellosillo et al. 2013; Okazaki and Saito 2014). Most literature associated with oxylipin production is in relationship to biotic stress factors and 13-Lipoxygenases. Current knowledge has not integrated 9-

LOXs into the network of drought stress related genes and the knowledge of oxylipin profiles produced by 9-LOXs is limited.

1.2 Lipid Biosynthesis and Fatty Acid Anabolism and Catabolism

Lipids are a diverse group of organic molecules that are insoluble in water and are responsible for a wide range of functions, some are only recently discovered but predominantly use for energy storage. This diverse group includes fats, oils, phospholipids, fatty acids, triacyglycerol's, glycolipids, sphingolipids, and steroids upon many others. In animals, when there is an oversupply of dietary carbohydrates, the excess carbohydrates are converted to triglycerides. This involves the synthesis of fatty acids from acetyl-CoA and the esterification of fatty acids in the production of triglycerides, a process called lipogenesis. Fatty acids are made by fatty acid synthases that polymerize then reduce acetyl-CoA units. The acyl chains in the fatty acid are extended by a cycle of reactions that add an acetyl group, reduce it to an alcohol, dehydrate it to an alkene group then further reduce it to an alkane group. The enzymes of fatty acid biosynthesis are divided into two groups, in animals and fungi all these fatty acid synthase reactions are carried out by a single multifunctional protein; (Chirala and Wakil 2004; Ohlrogge and Browse 1995) while in plant plastids and bacteria separate enzymes perform each step in the pathway (Ohlrogge and Browse 1995). Fatty acids provide a wide range of functions and purposes within cell biology. Fatty acids can be used to generate energy or for constructing phospholipids, messenger molecules, hormones and a variety of other biomolecules (Neitzel 2010; Feussner and Wasternack

2002). Catabolism of membrane lipids is carried out by the initial liberation of the fatty acid chain by cytosolic phospholipases; which cleave the fatty acid chain from the glycerol group.

Beta-oxidation is the metabolic process, in which fatty acids are broken down in the mitochondria and/or in peroxisomes to generate acetyl-CoA. Fatty acids are then oxidized by a mechanism that is similar to the reversal of the process of fatty acid biosynthesis. Two-carbon fragments are removed sequentially from the carboxyl end of the acid after the following steps of dehydrogenation, hydration, and oxidation to form a beta-keto acid; which are then split by means of thiolysis (Vishwanath 2016). The acetyl-CoA which is ultimately converted into ATP, CO_2, and H_2O using the citric acid cycle (CAC) and electron transport chain. Unsaturated fatty acids require specific enzymatic steps for degradation.

The most studied PUFA release processes from the plant cellular membrane are those from thylakoidal galactolipids in plastids mediated by lipases DGL and DAD1 (Hyun and Lee 2008). Resulting PUFAs are likely substrate of plastidal 13-LOX, and directed to JA and GLV biosynthesis. The mechanism of PUFA release in cytoplasm is poorly understood in plant, but it is likely mediated by cytosolic phospholipases. Cytosolic Phospholipase A_2 cleaves polyunsaturated fatty acids from the glycerol group of the phospholipid. Linoleic acid and α-linolenic acid are liberated by endogenous $cPLA_2$ stored in Patatin-like-proteins (Canonne et al. 2011; Hendriks et al. 1991; Feys et al. 2005; Cacas et al. 2009; Senda et al. 1996). The released PUFAs likely serve as substrates for cytosolic LOX isoforms.

1.3 What are lipoxygenases? Isoform distinction, and Oxylipin Products

Lipoxygenases are non-heme, iron dioxygenases, most of which catalyze the stereo- and regio- specific hydroperoxidation of polyunsaturated fatty acids (PUFAs) within lipids (Feussner and Wasternack 2002; Brash 1999). Lipoxygenases make up a large family of lipid oxidizing enzymes in the kingdom of Eukarya. Lipoxygenases are all similar in their structure and overall function. There are two main domains of the lipoxygenase proteins. The distinctive PLAT/LH2 domain, a beta barrel in the N-terminal portion of the LOX protein. The PLAT domain is a structurally conserved domain associated with membrane binding and lipid association. It is a beta-sandwich composed of two beta-sheets made up of four beta strands that run antiparallel to each other, with three calcium binding loops exposed on the exterior surface of the beta barrel (Newcomer and Brash 2015; Eek et al. 2015).

The second domain and catalytically active portion of the lipoxygenase protein is the lipoxygenase domain. The structure is also relatively conserved across Eukarya in specific motifs (Newcomer and Brash 2015). There are a few structures and functions within the lipoxygenase domain. The most identifiable is the iron binding catalytic center. The iron binding center provides the function of dioxygenating cis, cis 1-4 pentadiene linoleic and α-linolenic fatty acids in plants for eicosanoid and oxylipin production.

There are two double bonded carbon positions in which plant lipoxygenase catalysis can occur. The 9-carbon position and/or the 13-carbon position of (linoleic or α-linolenic) fatty acids. Plant lipoxygenases catalyze at three of the four available

positions (9R, 9S, and 13S) (Newcomer and Brash 2015; Egmond et al. 1972; Coffa et al. 2005). Position specificity in the lipoxygenase reaction plays a key role in overall oxylipin production and differentiation. The identification for oxidation on linoleic and α-linolenic acid is based on the regio and stereospecficity. Positioning the specific site of the PUFA in the lipoxygenases is dependent on a few key factors. The first is a shifting so the fatty acid can slide to different depths of the active site and expose a selected pentadiene for its reaction with the catalytic iron center (Newcomer and Brash 2015; Egmond et al. 1972; Kuhn et al. 1990). The second factor, is proper head-to-tail orientation of the substrate (Newcomer and Brash 2015). The 9 and 13 carbon positions are on opposite ends it is at this point that either pro-R or pro-S hydrogen is abstracted from the C11 position. Finally, the access of O_2 to the specific end of the reacting pentadiene is the ultimate determinant of the pro-R or pro-S specificity (Newcomer and Brash 2015; Brash 1999; Kuhn et al. 1990; Coffa and Brash 2004).

After lipoxygenase catalysis, downstream pathways such as Allene Oxide Synthase (AOS), and Hydroperoxide Lyase (HPL), play an essential enzymatic role in mediating the products of LOX reactions to oxylipin products. Jasmonic acid is one of the most well characterized oxylipins. JA biosynthesis is formed through the Allene Oxide Synthase, a cytochrome P450 enzyme; which converts 13(S)-hydroperoxylinolenic acid to 12,13-epoxylinolenic acid (Song et al. 1993). Specific plastid Allene Oxide Synthase(s) then cyclize to produce cis-(+)-OPDA (Song et al. 1993; Borrego and Kolomiets 2016). Cis-(+)-OPDA is then reduced by 12-

oxophytodinoate reductase 7/8, in maize, or 12-oxophytodinoate reductase 3, in arabidopsis to produce jasmonic acid (Borrego and Kolomiets 2016).

There is however, great diversity of oxylipin products in plants. Some of the most well studied are volatiles. Green leaf volatiles (GLVs), or C_6 volatiles play an essential role in plant-plant interactions as well as plant-insect interactions. GLVs are most frequently associated with two types of chemical interaction; the first being plant-plant interactions; which act as a priming communication under pathogen attack or abiotic stress to communicate with surrounding plants to modify physiological responses. (Vickers et al. 2009; Scala et al. 2013; Matsui et al. 2012; Bruce and Pickett 2011; Yamauchi et al. 2015). The second being plant-insect positive interactions. GLVs are released during insect herbivory, and other pathogen attack to mediate damage. This occurs in different ways. One way is the GLVs act as defensive compounds aimed at deterring herbivores or slowing the progressing of pathogens (War et al. 2011; Moraes et al. 2001; Bruce and Pickett 2011; Nakamura and Hatanaka 2002). Another way is by chemical attractant or beneficial insects, predators of the herbivores attacking the plants (Wei et al. 2007; Bruce and Pickett 2011). While GLV C_6 volatile interactions may be more understood, C_5 volatile functionality and formation are still relatively unknown.

CHAPTER II

ISOFORM-SPECIFIC SUBCELLULAR LOCALIZATION OF ZEA MAYS LIPOXYGENASES AND OXO-PHYTODIENOATE REDUCTASE 2*

1. Introduction

Oxylipins are a group of diverse lipid hydroperoxide compounds produced from polyunsaturated fatty acids, namely, linoleic (18:2) and linolenic acids (18:3) (Feussner and Wasternack, 2002). Plants collectively produce an estimated 650 molecular species of oxylipins with many exhibiting hormone-like signaling or direct antimicrobial activities (Borrego and Kolomiets, 2016). Some of plant oxylipins including jasmonic acid (JA), conjugate dienoic acids, and volatile aldehydes like green leaf volatiles (GLV) are well characterized (Sofo et al., 2004). Certain oxylipins are highly reactive and toxic to the host cells, others function as signal molecules in plant defense reaction against biotic and abiotic stresses (Wang and Yang, 2005; Xue et al., 2008; Mueller and Berger, 2009; Hou et al., 2016; Wasternack and Strnad, 2016; Lim et al., 2017). The prototypical plant oxylipin signal molecules are JA and its derivatives produced via octadecanoid pathway, collectively called jasmonates (Farmer and Ryan, 1992; Koiwa et al., 1997).

---

*Reprinted with permission from "Isoform-specific subcellular localization of Zea mays lipoxygenases and oxo-phytodienoate reductase 2" Tolley JP, Nagashima Y, Gorman Z, Kolomiets MV, Koiwa H. 2018. Plant Gene 13:36-41.

Production of oxylipins likely starts with a release of polyunsaturated fatty acids from membrane lipids. In the case of JA biosynthesis, linolenic acid from plastidial membrane galactolipids are released by the function of conserved plastidial galactolipases (Ishiguro et al., 2001; Hyun et al., 2008; Ellinger et al., 2010). Linolenic acid released to the stroma undergoes a 7-step conversion in plastid (lipoxygenase [LOX], allene oxide synthase, allene oxide cyclase) and peroxisome (oxo-phytodienoate reductase [OPR]) and three rounds of beta-oxidations to produce JA (Schaller, 2001). Resulting JA could be esterified to produce a volatile methyl-jasmonate, which can function in interplant signal communications (Farmer and Ryan, 1990; Tamogami et al., 2008), or conjugated with amino acids including biologically active jasmonate, JA-Ile (Staswick and Tiryaki, 2004).

Lipoxygenases (LOXs) (linoleate: oxygen oxidoreductase, EC 1.13.11.12) are a family of nonheme, iron-containing enzymes that catalyze the first step of converting polyunsaturated fatty acids derived from membrane lipids to oxylipins (Feussner and Wasternack, 2002). Plant lipoxygenase consists of 2 domains, a C-terminal catalytic domain (lipoxygenase domain) and an N-terminal PLAT/LH2 (Polycystin-1, Lipoxygenase, Alpha-Toxin / lipoxygenase homology 2) domain found in many lipid associated proteins (Bateman and Sandford, 1999). Two different plant LOX subgroups exist, 9-LOX and 13-LOX, based on the position specificity for the incorporation of the molecular oxygen into these fatty acids at C9 or C13 (Brash 1999). Functions of plant 13-LOX have been studied extensively in both monocots and dicots. All plant 13-LOXs characterized to date accumulated in plastids, and some of them were shown to function

in the production of jasmonate (Acosta et al., 2009; Chauvin et al., 2013) and GLV (Christensen et al., 2013). By contrast, little is known about the pathways mediated by each 9-LOX isoform. Most of 9-LOX proteins reported lack plastid targeting signals and likely function outside of the plastids, suggesting that different subcellular compartments other than plastids are responsible for the production of distinct sets of oxylipins (Wardale and Lambert, 1980; Vernooy-Gerritsen et al., 1984; Tranbarger et al., 1991; Matsui et al., 1992; Nalam et al., 2012).

The genome of monocot *Zea mays* cultivar B73 contains 12 isoforms of *LOX* genes, which represent six 13-LOXs and six 9-LOXs (Borrego and Kolomiets, 2016). In addition, maize, sorghum, and few other grasses harbor a unique monocot-specific LOX isoform, LOX6. LOX6 lacks an activity to oxidize fatty acids but functions as a hydroperoxide lyase that cleaves 13-LOX-derived hydroperoxide of linolenic acid into 13C- and 5C-containing oxylipins (Gao et al., 2008). Previous studies determined functions of maize 13-LOX paralogues in the production of JA (TS1/LOX8), and GLV (LOX10) (Acosta et al., 2009); (Christensen et al., 2013). As for maize 9-LOX homologs, genetic analysis suggested that oxylipins produced via different 9-LOX isoforms differentially impact plant-microbe and nematode interactions (Gao et al., 2009; Constantino et al., 2013; Christensen et al., 2014; Wang et al., 2017). By contrast, our understanding is still obscure concerning the mechanism of how 9-LOX functions are integrated into different branches of the oxylipin pathway (Christensen et al., 2015), and how plants differentially activate different 9-LOX pathways and subsequent signaling. As a first step to obtain molecular insight of maize 9-LOX homologs, I

conducted a systematic survey of subcellular localization using fluorescent protein (GFP) tagging approach. Four 9-LOX/LOX6 and one OPR proteins were fused to GFP in different configurations, and their subcellular localization patterns were determined using maize and Arabidopsis hosts. The data obtained from the analysis revealed surprisingly diverse localization profiles of individual 9-LOX isoforms suggesting that compartmentation of different oxylipin biosynthesis branches extends beyond the plastidial 13-LOX/non-plastidial 9-LOX paradigm.

2. Materials and Methods

2.2.1 *Preparation of expression cassettes for maize lipoxygenases*

Primers used for the PCR reactions were listed in Table S1. PCR fragments for LOX/OPR coding region were prepared by PCR using primer pairs (LOX2, 1444/1445/; LOX4 ,1428/1429; LOX6, 1430/1431; LOX12, T1 /T2; OPR2,1432/1433) and cDNA clones encoding LOX2 (ZM_BFc0165N03) LOX4 (ZM_BFc0171G14), LOX6 (Gao et al., 2008), LOX12 (Christensen et al., 2014), and OPR2 (p0010.cbpbi09 provided by Pioneer- a DuPont Company) as templates.

The PCR products were then introduced into Gateway entry vectors (pEnSOTG) (Bang et al., 2006) by SLiCE (Seamless Ligation Cloning Extract) homologous recombination cloning (Zhang et al., 2012). For internally tagged TP-mCherry-LOX6, cDNA fragments were prepared using primer pairs (1435 /1436, 1434/1437**,** 1438 /1437), and SLiCE reaction was prepared using three fragments and pEnSOTG digested with NcoI/NotI. After completion of the SLiCE reaction, each mixture was treated with Proteinase K at 37°C for 10 min and used for *E.coli* transformation by electroporation.

To prepare fusion proteins using monomeric GFP, pEnSOTG was modified to pEnSOmG by ligating a PCR fragment for mGFP (primer pair 922/923) and NcoI/NotI-digested pEnSOTG. LOX-mGFP expression cassettes were prepared as described above for LOX-GFP.

2.2.2 *PLAT/LH2 domain deletion constructs:*

Deletion constructs were generated using pEnSO-LOX4-mGFP. LOX4Δ2 and Δ6 were prepared by digesting pEnSO-LOX4-mGFP with XcmI/NcoI (Δ2) and RsrII/XcmI (Δ6), and subsequent blunting and self-ligation. For LOX4 Δ9 and Δ11, cDNA fragments containing deletions were prepared by PCR using primer pairs (LOX4Δ9, T32/T33; LOX4Δ11, T34/T35) and ligated to pEnSO-LOX4-mGFP digested with RsrII/XcmI for Δ9, or RsrII/XhoI for Δ11.

2.2.3 *Protoplast Transfection Assay:*

Protoplast transfection of maize cultivar B73 was performed using the polyethylene glycol (PEG)-mediated method (Jeong et al., 2013) with modifications. Maize seedlings were germinated under 16h light/8 hour dark condition then were moved under the dim light and kept for three days before the harvest. The middle part of the leaf blades was harvested and used for the protoplast preparations. All protoplasts were transfected using 10μg of purified plasmid and cultured for 12 hours at 25°C. Confocal microscopy images were collected using Nikon FN1 C1si.

2.2.4 *Arabidopsis transformation and selection:*

LOX/OPR-GFP/mCherry entry plasmids were recombined with pMDC99 (Curtis and Grossniklaus, 2003) using Gateway LR clonase (Thermo Fisher) according to the

manufacturer's protocol. Agrobacterium-mediated transformation and selection of *Arabidopsis thaliana* Col-0 were performed as described previously (Rips et al., 2014).

2.2.5 *Tonoplast isolation*

The 35-day-old leaf tissues of stable transgenic Arabidopsis lines overexpressing GFP-LOX4/5 were used to isolate vacuoles as described (Robert et al., 2007). The isolated intact vacuoles were observed using the confocal microscope.

3. Results

2.3.1 *Preparation of GFP/mCherry reporter gene for LOX/OPR subcellular localization*

In contrast to the observations that enzymes related to 13-LOX-derived oxylipin biosynthesis possess a clear plastid- or peroxisome-targeting (as in OPR3) signal, many 9-LOXs lack obvious targeting sequence making bioinformatics prediction of their subcellular localization difficult. To empirically determine the localization of maize 9-LOX family proteins in live cells, expression plasmids containing LOX-XFP fusion cassettes were prepared. In addition to 9-LOXs, OPR2, another unusual oxylipin pathway enzyme lacking peroxisome targeting signal (Zhang et al., 2005) was included in the analysis. Expression plasmids containing LOX/OPR with C-terminally fused GFP for protoplast transfection were prepared using the pEnSOTG vector (Figure 1). To ensure expression in maize protoplasts, expression of reporter genes was driven by the superpromoter (Ni et al., 1995). LOX and OPR2 were expressed as fusions to GFP(S65T) encoded by pEnSOTG. For isoforms that showed punctate or membrane-localized profiles with GFP(S65T), the analysis was repeated with monomeric-GFP (mGFP) to avoid potential aggregation caused by GFP-dimerization artifact (Segami et al., 2014). In our hands, GFP(S65T)- and mGFP- fusion constructs produced indistinguishable results. For LOX6, whose N-terminal region showed a weak feature for the plastid transit peptide, additional configuration, TP-mCherry-LOX6, was prepared, inserting mCherry between the predicted transit peptide and the PLAT domain of LOX6. Transformation of maize mesophyll protoplasts was performed using above expression cassettes in pEntr2B vector either directly or after the LR recombination with

a high-copy number vector pBluescript-GW. Stable Arabidopsis transgenic plants were prepared using binary vectors produced after LR recombination with pMDC99 binary vector.

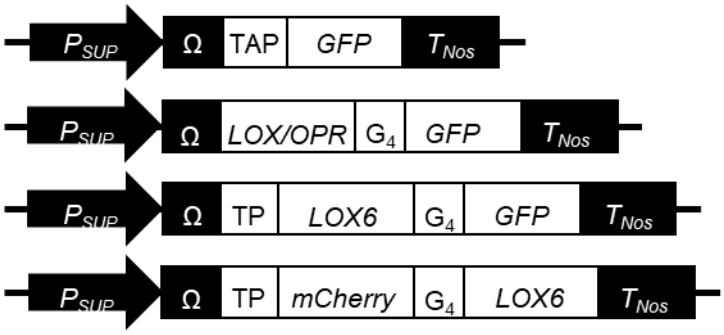

Figure 2-1. Schematic drawing of expression cassettes for GFP/mCherry-tagged LOXs and OPR. P_{SUP}, superpromoter; **Ω**, tobacco mosaic virus omega sequence; G_4, Glycine Linker; GFP, green fluorescence protein; TAP, TAP-tag; TP, transit peptide of LOX6; T_{nos}, *NOS* terminator.

2.3.2 *Cytoplasmic localization of LOX2/OPR2*

Figure 2 shows representative images of maize protoplasts and Arabidopsis transgenic plants expressing LOX2-GFP and OPR2-GFP reporters, as well as GFP-vector and untransformed controls. For ZmLOX2-GFP and OPR2-GFP, 200 out of 200 GFP-positive protoplast samples produced GFP signals throughout the cells including nuclei similar to GFP-vector-control, suggesting its cytoplasmic accumulation. The results were reproduced in stably transformed Arabidopsis root tissues.

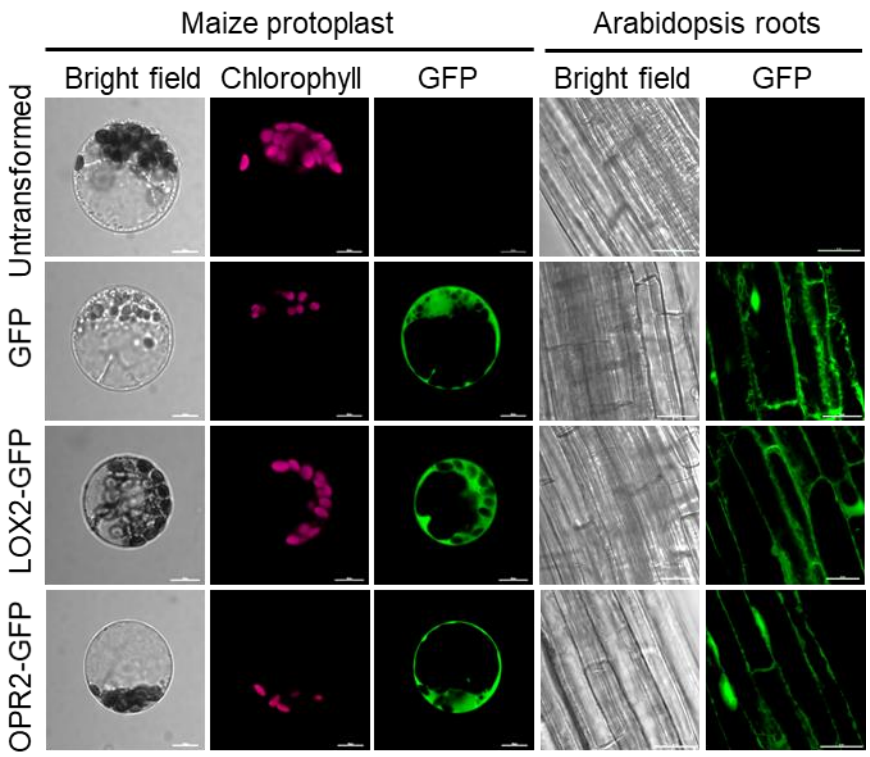

Figure 2-2. Maize protoplasts and Arabidopsis roots expressing LOX2-GFP and OPR2-GFP. Maize protoplasts were transfected with 10 μg expression plasmid DNA and were observed 14 hours after the transformation. Roots of stably transformed Arabidopsis plants (T2 generation) grown in vitro were observed 7 days after germination. Bars indicate 10 μm.

2.3.3 *LOX12 accumulates in unidentified intracellular structures*

Fluorescent signals from LOX12-GFP was localized to small particle domains in maize protoplasts (Figure 3). These subcellular domains neither resembled typical organelles like Golgi apparati/plastids/mitochondria nor overlap with markers for trans-Golgi network or peroxisome. In Arabidopsis roots, LOX12-GFP signals were observed from cellular bodies of varying shape and size depending on different transgenic lines and on ages of the plants. In young roots, LOX12-GFP signals accumulated in small

irregular-shaped bodies (1-3μm) or in a large (10 μm) body adjacent to nuclei. These observations suggested that LOX12 formed aggregates in cytoplasm and possibly targeted to aggresome-like structures (Zaarur et al., 2008).

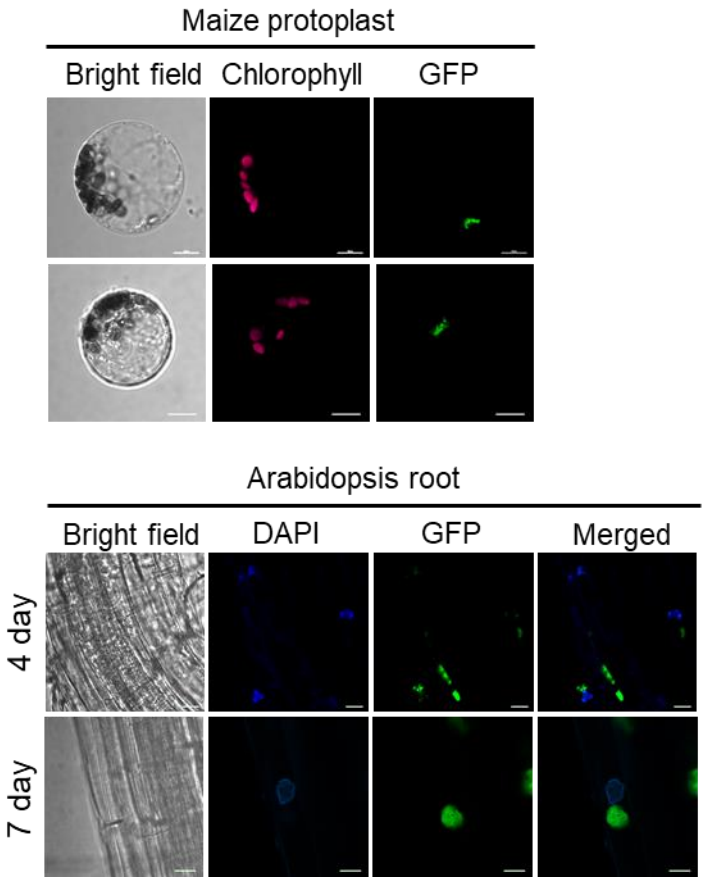

Figure 2-3. Maize protoplasts and Arabidopsis roots expressing LOX12-GFP. Maize protoplasts were transfected with 10 μg expression plasmid DNA and were observed 14 hours after the transformation. Roots of stably transformed Arabidopsis plants (T2 generation) grown in vitro were observed 4 and 7 days after germination. Nuclei were stained with 4,6-Diamidino-2-phenylindole. Bars indicate 10 μm.

2.3.4 *Plastid localization of LOX6*

Expression of LOX6-GFP in maize protoplasts produced GFP labels inside of plastids in all 200 protoplasts scored (Figure 4). Inside the plastids, the pattern of GFP signals did not match with that of the chlorophyll signals, suggesting LOX6 accumulated in the stromal space. The accumulation pattern was configuration-independent, as a similar profile was observed when mCherry was inserted between the putative LOX6 transit peptide and the mature LOX6. (Figure 4, mCh-LOX6). In Arabidopsis roots, LOX6-GFP accumulated in particle-like organelles. These particles accumulated chlorophyll under constant light, confirming their identity as plastids. In Arabidopsis leaf tissues, LOX6-GFP localization showed dichotomies. Both locations were chlorophyll-positive, but one showed grouped almond-shaped chloroplasts which are typical of mesophyll cell chloroplasts. Also, strong GFP signals were observed in smaller, isolated plastids in pavement cells (Barton et al., 2016). Strong GFP signals from stroma-rich pavement cell plastids further supported LOX6 accumulation in the stroma (Barton et al., 2016).

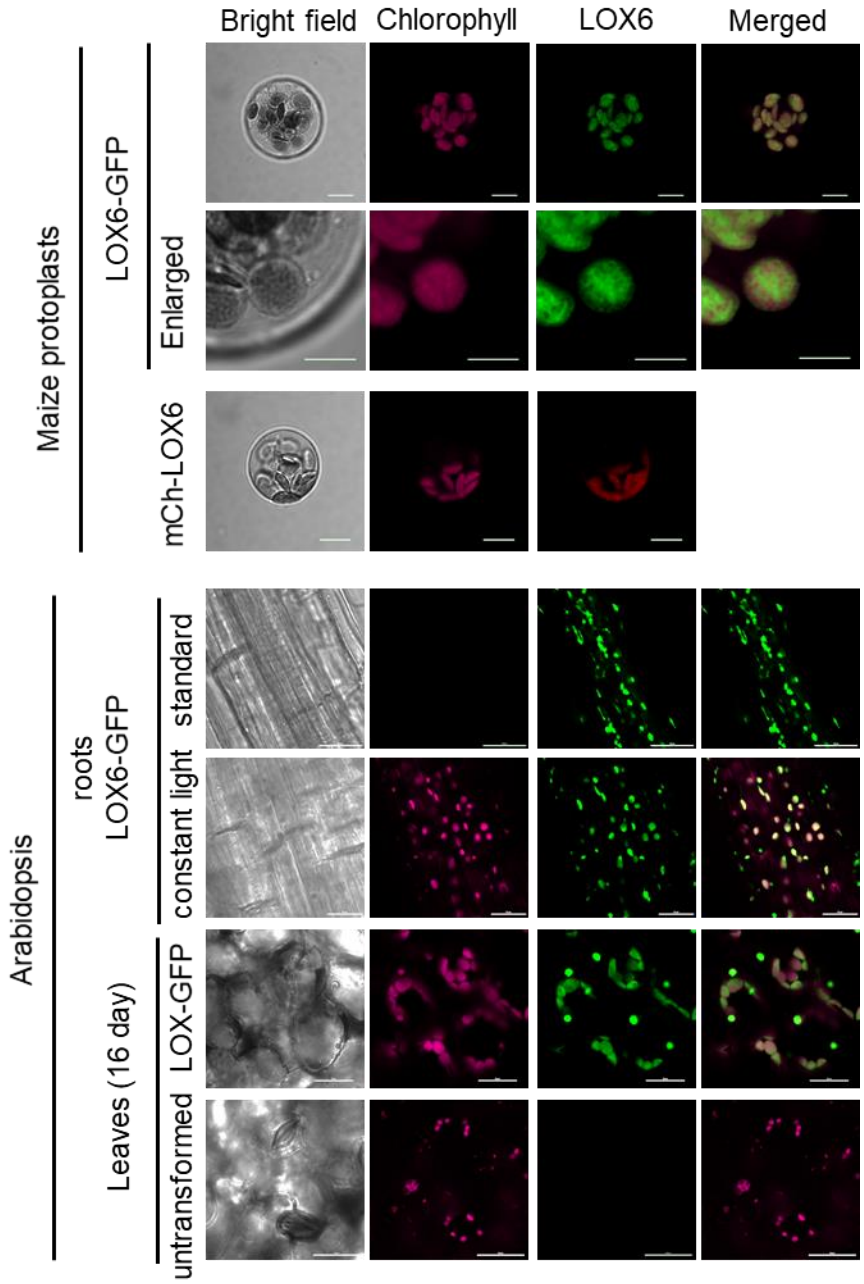

Figure 2-4. Maize protoplasts and Arabidopsis plants expressing LOX6-GFP or mCherry(mCh)-LOX6. Maize protoplasts were transfected with 10 µg expression plasmid DNA and were observed 14 hours after the transformation. Roots of stably transformed Arabidopsis plants (T2 generation) grown in vitro were observed 10 days after germination (standard). Chlorophyll accumulation in roots was induced by growing plants under the constant light for 22 days. Bars indicate 10 µm for protoplasts and roots and 20µm for leaves.

2.3.5 *LOX4 was localized to the cytoplasm and tonoplasts*

LOX4-GFP signals were observed in the cytoplasm as well as tonoplasts (Figure 5A). 189 of 200 scored protoplasts produced the tonoplast labels. Remaining samples produced strong cytoplasmic GFP signals without clear tonoplast labels. In Arabidopsis roots, LOX4-GFP labeled intracellular membranes similar to one observed with maize protoplasts. Using GFP or mGFP, or fusing GFP to N-termini or C-termini did not change the localization pattern (data not shown). To confirm that these intracellular membranes represent tonoplasts, I isolated vacuoles from leaf mesophyll cells expressing LOX4-GFP as well as vector control plant expressing cytoplasmic GFP. As shown in Figure 5B, mesophyll protoplasts isolated from transgenic Arabidopsis lines reproduced the GFP labeling pattern seen in the maize protoplasts. Subsequently, vacuoles were isolated from protoplasts according to the method described by (Robert et al. 2007). The GFP signals were specifically detected in the vacuoles isolated from LOX4-GFP protoplasts but not from GFP-vector protoplasts. These results established that LOX4 was targeted to the tonoplasts.

LOX4 does not contain clear targeting motifs for the subcellular localizations. To determine if specific tonoplast targeting motifs were present in LOX4, I prepared internal deletion series of LOX4-mGFP expression cassettes and expressed in maize protoplasts. Figure 6 shows representative images for each construct. In summary, full-length LOX4 was required for the tonoplast targeting. The PLAT domain and the lipoxygenase domain by themselves were not sufficient for the tonoplast localization.

Instead, GFP signals were observed in the cytoplasm for the all deletion constructs tested.

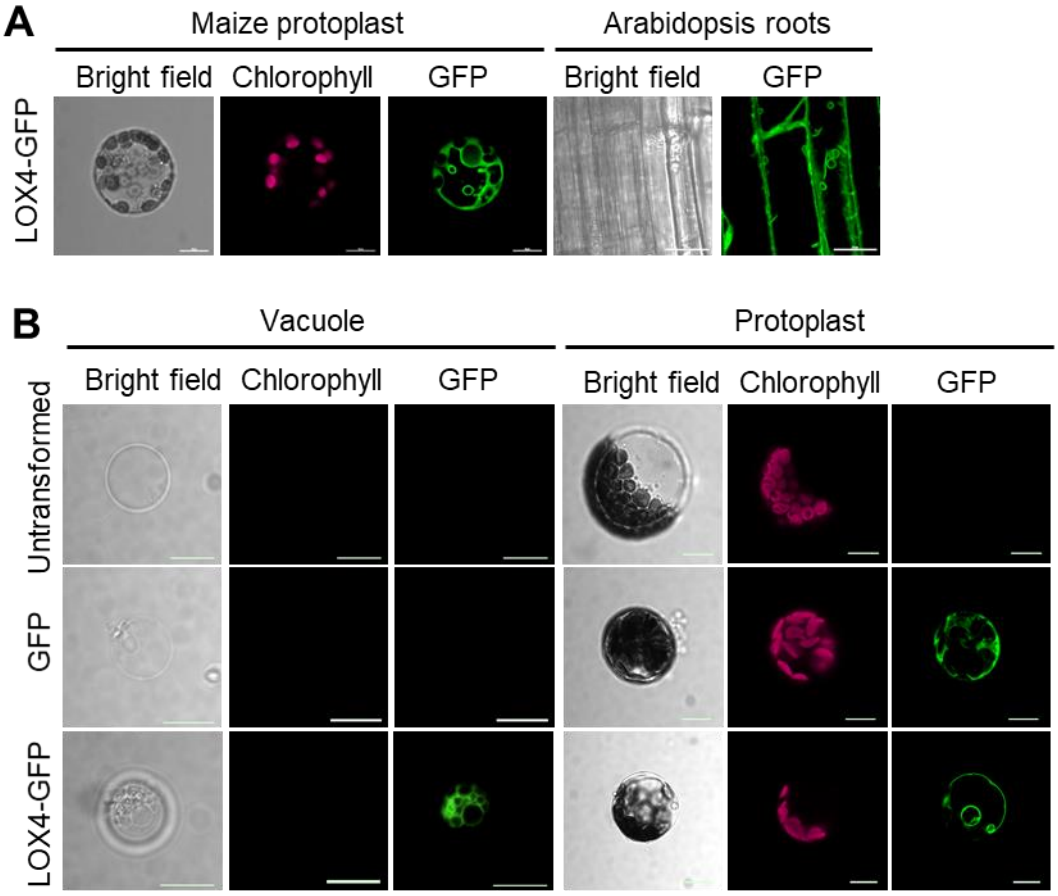

Figure 2-5. Maize protoplasts and Arabidopsis plants expressing LOX4-GFP. A) Maize protoplasts were transfected with 10 µg expression plasmid DNA and were observed 14 hours after the transformation. Roots of stably transformed Arabidopsis plants (T2 generation) grown in vitro were observed 10 days after germination. B) Vacuoles isolated from Arabidopsis mesophyll protoplasts stably expressing LOX4-GFP. Untransformed plants and plants expressing unfused GFP were used for control. Vacuoles were isolated from protoplasts prepared from leaves of 35-day-old plants. Spherical intravacuolar structures were uniquely observed for LOX4-GFP in both maize and Arabidopsis transformants. Bars indicate 10µm.

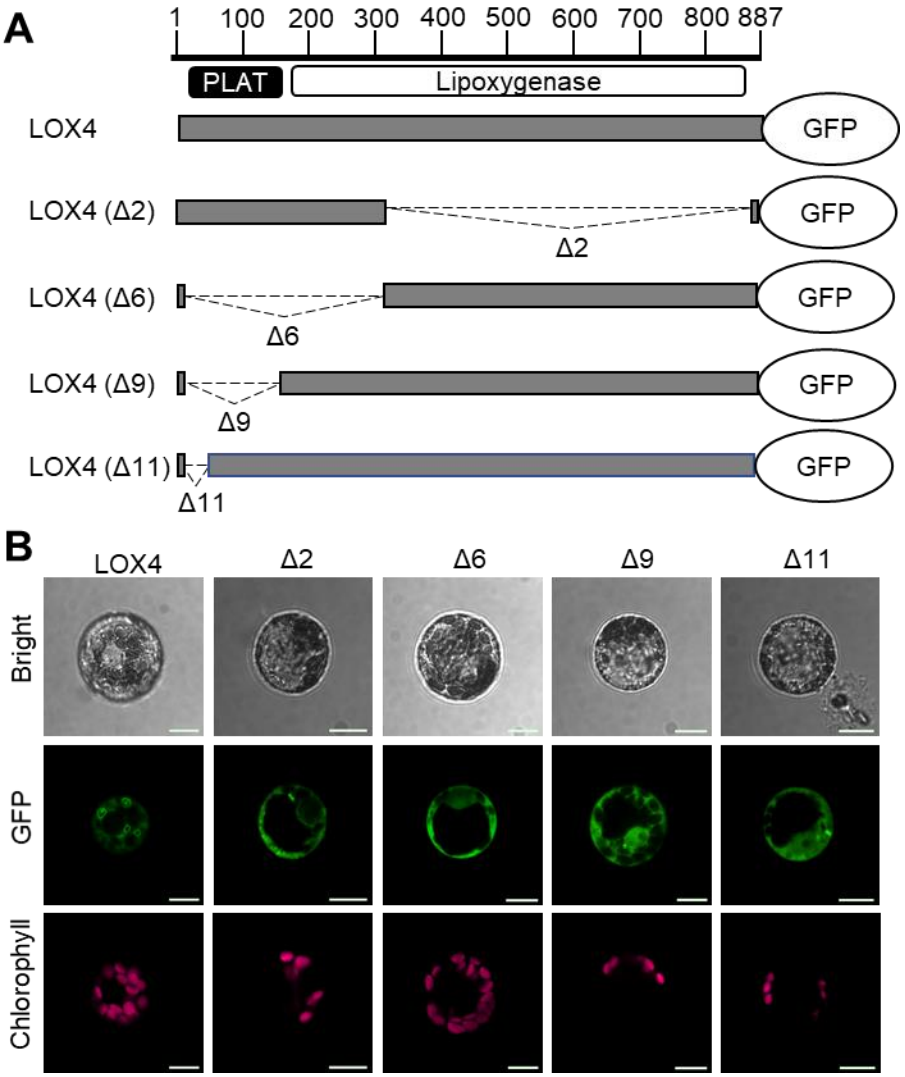

Figure. 2-6. Neither the lipoxygenase domain nor the PLAT/LH2 domain of LOX4 were sufficient for tonoplast localizations. A) schematic drawing of LOX4-GFP serial deletion variants. B) Maize protoplasts expressing LOX4-GFP variants. Maize protoplasts were transfected with 10 µg expression plasmid DNA and were observed 14 hours after the transformation. Bars indicate 10 µm.

4. Discussion

9-LOXs are responsible for the production of 9-hydroperoxides of linoleic and linolenic acids, which is an early step reaction feeding the seven branches of the LOX pathway for biosynthesis of diverse 9-LOX-derived oxylipins (Feussner and Wasternack, 2002). Using maize and Arabidopsis hosts, this study revealed the diversity of subcellular localization profile of maize 9-LOX subfamily and OPR2 proteins. I found accumulations of maize 9-LOXs in plastids, cytoplasm, tonoplast, and unidentified particles, suggesting maize 9-LOX-derived oxylipin biosynthesis was associated with different subcellular compartments. Most of the locations were relatively easy to match with known subcellular components. However, the identity of the LOX12-positive structure was not clear. Plastid localization of LOX6 was consistent with previous plastid import assay data (Gao et al., 2008) and presence of a TP-like stretch in LOX6 N-terminus. LOX6 is an unusual enzyme with hydroperoxy lyase activity toward 13-hydroperoxide of linolenic acid, but with no detectable lipoxygenase activities (Gao et al., 2008). Based on its localization, LOX6 likely functions downstream of plastid localized 13-LOX isoforms like LOX8 and LOX10 in GLV production pathway (Duan et al., 2005; Christensen et al., 2013).

The most striking finding in this study was the tonoplast localization pattern of LOX4. This is distinct from soybean vacuolar lipoxygenases, which are known as vegetative storage proteins and accumulate in the vacuolar lumen without forming membrane structures (Fischer et al., 1999). Although the intravacuolar spherical structures produced in LOX4 -GFP resembles "bulbs" reported for the dimer-forming

GFP that are targeted to tonoplasts (Segami et al., 2014), the structure was observed regardless of fusing LOX4 to conventional GFP or monomeric GFP. Also, unlike very strong signals from bulbs, the signal intensity from LOX4-GFP intravacuolar structures was not substantially higher than tonoplast GFP signals. Therefore, the structures observed with LOX4 -GFP were likely induced by expression of LOX4 itself, rather than by dimerization of GFP. Cytoplasm LOX4-GFP signals were often observed together with tonoplast signals. Maize LOX4 localization profiles were also distinct from two Arabidopsis 9-LOXs, plastidial AtLOX1 and cytoplasmic AtLOX5 (Nalam et al., 2012). Neither the lipoxygenase domain nor the N-terminal PLAT domain was sufficient for the tonoplast targeting of LOX4. However, a small deletion inside of PLAT/LH2 domain prevented the tonoplast location. Since LOX4-GFP signals were detected in the cytoplasm as well, tonoplast localization might occur after LOX4 was synthesized in the cytoplasm and formed native conformation. The recruiting mechanism for LOX4 likely recognizes a signal patch formed by multiple peptide segments, not a simple peptide motif, via protein-protein interactions.

Understanding isoform-specific localization is a step toward determining a specific mode of function for each 9-LOX. Although in vitro-enzymatic properties are similar for most isoforms, biological functions for 9-LOX isoforms are distinct. For example, LOX12 promotes JA production in response to pathogen infection (Christensen et al., 2014), whereas another 9-LOX, LOX3, suppresses JA, salicylic acid, and ethylene production in roots via biosynthesis of as yet unidentified oxylipin(s) (Gao et al., 2009; Wang et al., 2017). In the case of LOX4, despite a very high homology between LOX4

and LOX5, mutations in LOX4 and LOX5 produced opposite effects on host resistance against *Colletotrichum graminicola*, i.e., *lox4* mutants showed increased susceptibility, but *lox5* showed increased resistance (Park, 2011). Because LOX4 and LOX5 showed distinct expression profiles during development and host defense responses (Park et al., 2010), we propose incorporation of a specific 9-LOX isoform to specific downstream branches of the LOX pathway determines defense response of plants, and the tonoplast serves as a scaffold to assemble a specific pathogen-induced oxylipin biosynthesis pathway. Notably, another oxylipin pathway enzyme, CYP74C (9-hydroperoxide-specific allene oxide synthase) from petunia (Xu et al., 2006), were localized to tonoplast, supporting the tonoplast-localized oxylipin production pathways. Localization-assisted tracking will help mapping integrated network of oxylipin pathway branches for further understanding of bioactive 9-LOX-derived oxylipins.

CHAPTER III

FUNCTIONS OF *ZEA MAYS* LIPOXYGENASE-6 ENDOGENOUSLY OVEREXPRESSED IN *ARABIDOPSIS THALIANA*

3.1 Introduction

Volatiles and chemical signaling are an important means of communication in the organic world, and plants are masters at chemical signaling (Kong et al. 2003). Because plants are sessile organisms and have limited ways to surviving in their environment's, plants have evolved a variety of strategies and biosynthetic pathways to uniquely adapt. One of the most important pathways of chemical communication in plants is via the lipoxygenase pathway. Lipases cleave poly-unsaturated fatty acids and then oxidized by plastid localized lipoxygenases. In *Zea mays*, lipoxygenase (LOX 10), which is a 13S-linoleate LOX and is the major source for producing intermediate of plant volatiles in maize (Christensen et al. 2013; Mochizuki et al. 2016). In Arabidopsis the homolog to ZmLOX10 is AtLOX2. These proteins di-oxygenate 18:3 α-linoleic acid to make 13-HPOT. 13-HPOT is then in cleavage reactions to produce volatile products. The hydroperoxide lyase (HPL) branch is well-characterized in plants and produces six-carbon volatiles by cleavage of 13-HPOT are used for a variety of direct, indirect defenses as well as other plant signaling interactions (Christensen et al. 2013). Plants also produce five-carbon volatiles, which are far less understood. The biosynthesis of C_5 volatiles are nearly identical to their close relative of six-carbon compounds, but the genes related to the biosynthesis, release, uptake and perception, and overall impact are not well understood (Mochizuki et al. 2016).

Among 12 maize LOX isoforms, LOX6 has unique primary sequence that deviate prototypical LOX isoforms. Previous study using bacterially-produced recombinant LOX6 suggested that LOX6 uses 13-HPOT as substrate and produce five-carbon products (Gao et al. 2008). LOX6 expression was highest in leaves, and LOX6 peptide was incorporated to plastid in in vitro transport assay. Plastid localization was further confirmed by LOX6 fused to GFP or RFP fusion in transfected maize protoplasts as well as in stable transgenic Arabidopsis plants (Tolley et al. 2017). These data suggested that LOX6 functions as a plastidal HPL rather than LOX in maize, in vivo data supporting this hypothesis is lacking. In this work, I characterized the LOX6 function in vivo using Arabidopsis transgenic plants overexpressing *ZmLOX6*.

3.2 Materials and Methods

Preparation of Expression Cassettes for maize lipoxygenases

To prepare expression plasmid for untagged LOX6, LOX6 cDNA clone (Accession # DQ335764) was amplified by PCR using a primer pair (1629 BluntLOX6F /1626 NotI-LOX6R). PCR products were then gel-purified and digested by NotI. pEnEOimGF3SGThsp vector was prepared by digestion with NcoI followed by blunting using *Pfu* polymerase, then was digested by NotI in order to accept ZmLOX6 PCR amplified product. Digested vector and ZmLOX6 PCR product were then ligated together using T_4 ligase for overnight at 4°C. Ligation reaction mix was then electroporated into DH10B competent cells. Positive clone was identified by colony PCR screening. Resulting pEnEOiLOX6Thsp was sequenced using primers (1159

IntseqF /1454 LOX6seqF1/1455 LOX6seqF2/T51 LOX6seqF3) to confirm the LOX6 sequence.

Arabidopsis transformations

LOX6 entry plasmids were recombined with pMDC99 using Gateway LR clonase (Curtis and Grossniklaus 2003) according to the manufacturer's protocol. Prior to the LR reaction, the entry plasmid was digested with AsiSI enzyme cutting in the middle of the kanamycin cassette. Linearized entry plasmid containing ZmLOX6 cassette was moved into destination vector pMDC99. Reaction mixture was set up in a 2.5µL reaction using 1.0µL entry plasmid, 0.5µL destination vector, 0.5µL of buffer, 0.5µL 1x TE, and 0.3µL LR clonase. Resulting pMDC99EOiLOX6Thsp was introduced into Agrobacterium tumefaciens strain GV3101 by electroporation, which was used for floral transformation of 4-week-old *Arabidopsis thaliana* (Col-0 and *rdr6-11* ecotypes) as described (Clough and Bent 1998). The T_1 Seeds were bulk-harvested from Agrobacterium-treated plants. Surface-sterilized T_1 seeds were plated on media containing 1/3x strength Peters 20-10-20 General Purpose, 0.75% agar 35µg hygromycin. Seeds were then stratified for 3 days at 4ºC. Plates were grown in the light at 25ºC for 2 days, then grown under low light conditions for seedlings to etiolate. Transformed seedlings were transferred to rescue media to grow for 2 weeks before transferred to soil.

Growth conditions for Arabidopsis

Arabidopsis seeds were sown on ¼ MS (Murashige and Skoog) media containing 1.0% sucrose, 1.5% agar, wrapped with 3M™ Micropore surgical tape

(https://www.3m.com/) and stratified for 3 days at 4ºC. Seeds were then germinated and seedlings were grown vertically at 25ºC with long-day conditions (16-hour day/8-hour night). 8-9 day-old seedlings were used for all experiments grown on 1/4MS media unless otherwise stated. Soil grown Arabidopsis was grown in LP5 potting medium (Sun Gro Horticulture, Bellevue, WA) or in a 1:1 ratio of Jolly Gardener C/GP and C/20 potting mix (https://jollygardener.com/) and grown in an environmental growth chamber at 24ºC (day)/22ºC (night), 60% relative humidity, with long-day conditions (16-hour day/8-hour night) 3-4 week-old plants were used for analysis unless otherwise stated.

RNA Extraction and RT-PCR and qPCR

Total RNA was extracted from 8-9 day-old seedlings, RNA extraction and Reverse transcription were done as described (Fukudome et al. 2014). Total RNAs were extracted using TRIzol reagent, followed by DNase I treatment to eliminate all DNA contamination. One microgram of total RNAs were converted to first-strand cDNA by GoScript® Reverse Transcriptase 74 (Promega, https://www.promega.com/). The reverse transcription products were analyzed using a LightCycler 480 (Roche Diagnostics, http://www.roche.com/) and Bullseye EvaGreen qPCR Mastermix (http://www.midsci.com). 18S rRNA (AT2G01010) was used as an internal control for normalization in qPCR. In RT-PCR experiments -Reverse Transcriptase was used as a control due to the heterologous nature of the maize gene in Arabidopsis. Primers used are listed in Appendix.

Chlorophyll Extractions

Total chlorophyll contents of Arabidopsis plants were extracted from leaf tissue and determined as described by (Aksoy et al. 2013; Hu et al. 2013). Total shoot tissues were soaked acetone for 3 days at -20ºC. 50 mg fresh tissues were extracted in 1 mL 80% (v/v). The supernatant was collected after centrifugation at 15000 g for 5 min at 4°C. Absorbance at 646.8 and 663.2 nm was measured by a spectrophotometer (Epoch Biotek micro plate reader spectrophotometer, https://www.biotek.com/). 200µL 80% (v/v) acetone was used as blank. Total chlorophyll content (chlA + chlB) was calculated as (7.15 A663.2 + 18.71 A646.8)/1000/Fresh weights of leaves.

Gas Chromatography/Mass Spectrometry

Leaves of 30-day old *Arabidopsis thaliana* leaves were cut into approximately 1 cm pieces. The pieces were quickly weighed out and approximately 3 g (4-6 plants) of tissue was placed into 800 mL jars for volatile collection. Volatiles were collected onto HaySepQ filter traps containing 80-100 mesh (Supelco) via dynamic airflow. The air flow through the system was approximately 1.5 L/min, and the air entering the system was filtered via activated carbon. Volatile collections lasted for 1 h. Volatiles were eluted off the HaySepQ filters with 250 µL of dichloromethane containing 100 µM of the internal standards, pentadecane and nonyl acetate. Samples were subsequently analyzed on an Agilent 7890B gas chromatograph connected to an Agilent 5977B quadrupole mass spectrometer. 2 µL of sample was injected splitless into a HP-5ms Ultra Inert column (Agilent). The inlet temperature was set to 240 °C for the duration of the run. The oven temperature was as follows: 40 °C hold – 2 min, 3 °C/min ramp to 160

°C, 15 °C/min ramp to 280 °C, 280 °C/min hold – 2 min. The solvent delay was 2.5 min. Analytes were fragmented by positive EI (230 °C – source, 150 °C – quadrupole, ionization energy – 70eV, scan range – 25-500 amu). Most compounds were identified based off of retention times and spectra of pure external standards purchased from Sigma-Aldrich. The compound 4-oxo-(*E*)-2-hexenal, (*Z*)-2-pentenyl acetate, 4-hydroxy-(*E*)-2-hexenal were identified based off matching of mass spectra and retention index (RI), calculated according to (Van Der Dool and Kratz 1963) in the NIST14 library. The compound tentatively referred to as (*Z*)-2-pentenal was identified by almost identical spectral matching to (*E*)-2-pentenal and a close retention proximity characteristic of (*E/Z*)-isomers of other lipoxygenase-produced volatiles. All volatiles were quantified based through the use of internal standards and external standards.

Aphid Choice Test Assay

Arabidopsis thaliana was grown in LP5 potting medium (Sun Gro Horticulture, Bellevue, WA) in growth chamber at 23ºC (day)/21ºC (night), 65% relative humidity and 12 hours light/12 hours dark photoperiod with a photosynthesis photon flux density of 85µMoles $m^{-2}s^{-1}$. For aphid choice tests, 3 to 4-week-old plants were used. Phloem sap-feeding green peach aphids *M. persicae* (from Dr. Keyan Zhu-Salzman's lab) were cultured on cabbage (*Brassica oleracea*) and maintained in an environmental chamber at 21ºC, 65% relative humidity, and 12 hour light/12 hour dark photoperiod (63 µMoles m-2s-1).

Statistical analysis

JMP statistical software was used for analyses for all data. One-way ANOVA was used for GC/MS analysis. The Chi-Squared test was used for the analysis of choice test insect assay.

3.3 Results

3.3.1 *Structure of LOX6*

In order to visualize the molecular characteristics of ZmLOX6, I compared LOX6 peptide sequence with other maize lipoxygenases as well as representative plant lipoxygenases using multiple sequence alignment by ClustralW2 program. The first assessment was to show differences in amino acid sequencing, particularly the C-terminus. There is a highly conserved motif in the C-terminus with the sequence (serine, isoleucine, serine, isoleucine). However, in ZmLOX6 the C-terminus motif is the amino acid composition of (serine, isoleucine, threonine, valine). Other highly conserved amino acid residues of lipoxygenase proteins which are essential for functionality of the catalytic iron binding are the histidine 554, histidine 559, histidine 746, and isoleucine 890, with the final isoleucine in all other lipoxygenase proteins being present but replaced in ZmLOX6 with a valine. Valine, threonine, and isoleucine are C-beta branching amino acids, and although rarely involved in protein function it can also play a role in substrate recognition. In particular, hydrophobic amino acids can be involved in binding/recognition of hydrophobic ligands, particularly lipids (Betts et al. 2003).

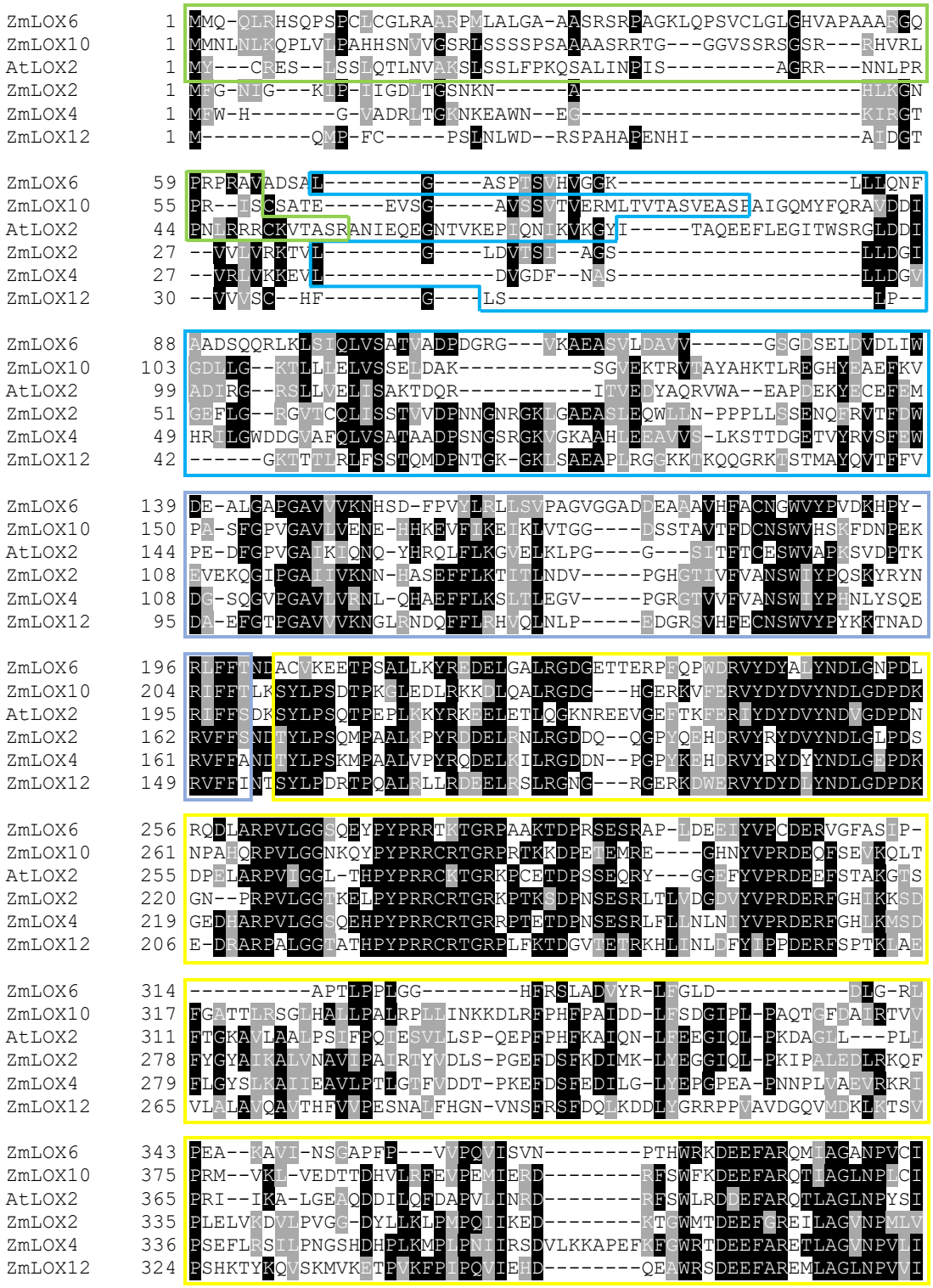
ZmLOX6
ZmLOX10
AtLOX2
ZmLOX2
ZmLOX4
ZmLOX12

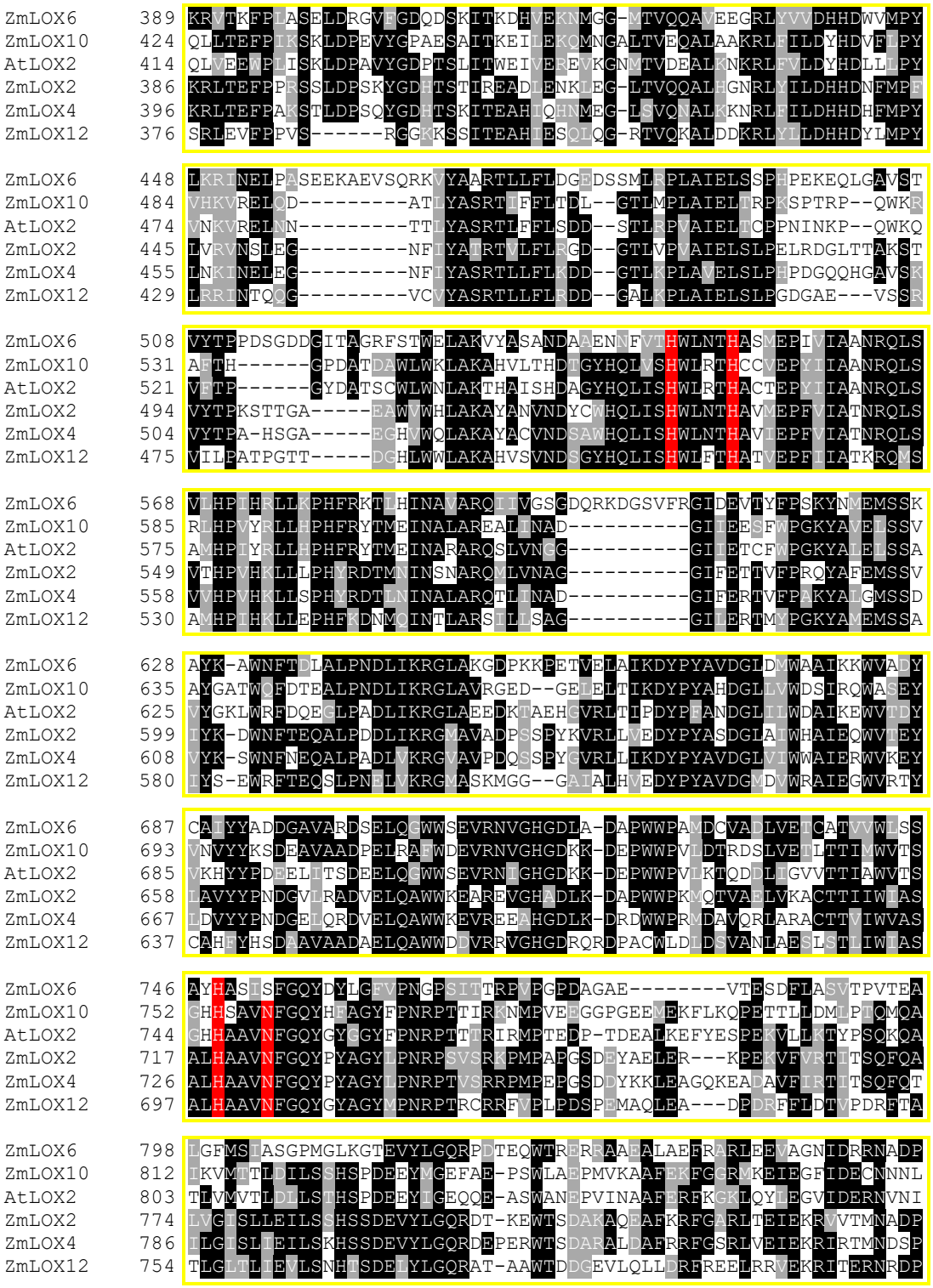
ZmLOX6 389 KRVTKFPLASELDRGVFGDQDSKITKDHVEKNMGG-MTVQQAVEEGRLYVVDHHDWVMPY
ZmLOX10 424 QLLTEFPIKSKLDPEVYGPAESAITKEILEKQMNGALTVEQALAAKRLFILDYHDVFLPY
AtLOX2 414 QLVEEWPLISKLDPAVYGDPTSLITWEIVERFVKGNMTVDEALKNKRLFVLDYHDLLLPY
ZmLOX2 386 KRLTEFPPRSSLDPSKYGDHTSTIREADLENKLEG-LTVQQALHGNRLYILDHHDNFMPF
ZmLOX4 396 KRLTEFPAKSTLDPSQYGDHTSKITEAHIQHNMEG-LSVQNALKKNRLFILDHHDHFMPY
ZmLOX12 376 SRLEVFPPVS------RGGKKSSITEAHIESQIQG-RTVQKALDDKRLYLLDHHDYLMPY
ZmLOX6 448 LKRINELPASEEKAEVSQRKVYAARTLLFLDGEDSSMLRPLAIELSSPHPEKEQLGAVST
ZmLOX10 484 VHKVRELQD---------ATLYASRTLFFLTDL--GTLMPLAIELTRPKSPTRP--QWKR
AtLOX2 474 VNKVRELNN---------TTLYASRTLFFLSDD--STLRPVAIELTCPPNINKP--QWKQ
ZmLOX2 445 LVRVNSLEG---------NFIYAIRTVLFLRGD--GTLVPVAIELSLPELRDGLTTAKST
ZmLOX4 455 LNKINELEG---------NFIYASRTLLFLKDD--GTLKPLAVELSLPHPDGQQHGAVSK
ZmLOX12 429 LRRINTQQG---------VCVYASRTLLFLRDD--GALKPLAIELSLPGDGAE---VSSR
ZmLOX6 508 VYTPPDSGDDGITAGRFSTWELAKVYASANDAAENNFVTHWLNTHASMEPIVIAANRQLS
ZmLOX10 531 AFTH------GPDATDAWLWKLAKAHVLTHDIGYHQLVSHWLRTHCCVEPYIIAANRQLS
AtLOX2 521 VFTP------GYDATSCWLWNLAKTHAISHDAGYHQLISHWLRTHACTEPYIIAANRQLS
ZmLOX2 494 VYTPKSTTGA-----EAWVWHLAKAYANVNDYCWHQLISHWLNTHAVMEPFVIATNRQLS
ZmLOX4 504 VYTPA-HSGA-----EGHVWQLAKAYACVNDSAWHQLISHWLNTHAVIEPFVIATNRQLS
ZmLOX12 475 VILPATPGTT-----DGHLWWLAKAHVSVNDSGYHQLISHWLFTHATVEPFIIATKRQMS
ZmLOX6 568 VLHPTHRLLKPHFRKTLHINAVARQIIVGSGDQRKDGSVFRGIDEVTYFPSKYNMEMSSK
ZmLOX10 585 RLHPVYRLLHPHFRYTMEINALAREALINAD----------GIIEESFWPGKYAVELSSV
AtLOX2 575 AMHPIYRLLHPHFRYTMEINARARQSLVNGG----------GIIETCFWPGKYAIELSSA
ZmLOX2 549 VTHPVHKLLLPHYRDTMNINSNARQVLVNAG----------GIFETTVFPRQYAFEMSSV
ZmLOX4 558 VVHPVHKLLSPHYRDTLNINALARQTLINAD----------GIFERTVFPAKYALGMSSD
ZmLOX12 530 AMHPIHKLLEPHFKDNMQINTLARSILISAG----------GILERTMYPGKYAMEMSSA
ZmLOX6 628 AYK-AWNFTDLALPNDLIKRGLAKGDPKKPETVELAIKDYPYAVDGLDMWAAIKKWVADY
ZmLOX10 635 AYGATWQFDTEALPNDLIKRGLAVRGED--GELELTIKDYPYAHDGLLVWDSIRQWASEY
AtLOX2 625 VYGKLWRFDQEGLPADLIKRGLAEEDKTAEHGVRLTIPDYPFANDGLILWDAIKEWVTDY
ZmLOX2 599 IYK-DWNFTEQALPDDLIKRGMAVADPSSPYKVRLLVEDYPYASDGLAIWHAIEQWVTEY
ZmLOX4 608 VYK-SWNFNEQALPADLVKRGMAVPDQSSPYGVRLLIKDYPYAVDGLVIWWAIERWVKEY
ZmLOX12 580 IYS-EWRFTEQSLPNELVKRGMASKMGG--GAIALHVEDYPYAVDGMDVWRAIEGWVRTY
ZmLOX6 687 CAIYYADDGAVARDSELQGWWSEVRNVGHGDLA-DAPWWPAMDCVADLVETCATVVWLSS
ZmLOX10 693 VNVYYKSDEAVAADPELRAIWDEVRNVGHGDKK-DEPWWPVLDTRDSLVETLTTIMWVTS
AtLOX2 685 VKHYYPDEELITSDEELQGWWSEVRNIGHGDKK-DEPWWPVLKTQDDLIGVVTTIAWVTS
ZmLOX2 658 LAVYYPNDGVLRADVELQAWWKEARFVGHADLK-DAPWWPKMQTVAELVKACTTIIWIAS
ZmLOX4 667 LDVYYPNDGELQRDVELQAWWKEVREEAHGDLK-DRDWWPRMDAVQRLARACTTVIWVAS
ZmLOX12 637 CAHFYHSDAAVAADAELQAWWDEVRRVGHGDRQRDPACWLDLDSVANLAESLSTLIWIAS
ZmLOX6 746 AYHASISFGQYDYLGFVPNGPSITTRPVPGPDAGAE--------VTESDFLASVTPVTEA
ZmLOX10 752 GHHSAVNFGQYHFAGYFPNRPTTIRKNMPVEEGGPGEEVEKFLKQPETTLLDMLPIQMQA
AtLOX2 744 GHHAAVNFGQYGYGGYFPNRPTTIRIRMPTEDP-TDEALKEFYESPEKVLLKTYPSQKQA
ZmLOX2 717 ALHAAVNFGQYPYAGYLPNRPSVSRKPMPAPGSDEYAELER---KPEKVFVRTITSQFQA
ZmLOX4 726 ALHAAVNFGQYPYAGYLPNRPTVSRRPMPEPGSDDYKKLEAGQKEADAVFIRTITSQFQT
ZmLOX12 697 ALHAAVNFGQYGYAGYMPNRPTRCRRFVPLPDSPEMAQLEA---DPDRFFLDTVPDRFTA
ZmLOX6 798 LGFMSIASGPMGLKGTEVYLGQRPLTEQWTRERRAAEALAEFRARLEEVAGNIDRRNADP
ZmLOX10 812 IKVMTTLDILSSHSPDEEYMGEFAE-PSWLAEPMVKAAFEKFGGRMKEIEGFIDECNNNL
AtLOX2 803 TLVMVTLDLLSTHSPDEEYIGEQQE-ASWANEPVINAAFERFKGKLQYLEGVIDERNVNI
ZmLOX2 774 LVGISLLEILSSHSSDEVYLGQRDT-KEWTSDAKAQEAFKRFGARLTEIEKRVVTMNADP
ZmLOX4 786 ILGISLIEILSKHSSDEVYLGQRDEPERWTSDARALDAFRRFGSRLVEIEKRIRTMNDSP
ZmLOX12 754 TLGLTLIEVLSNHTSDELYLGQRAT-AAWTDDGEVLQLLDRFREELRRVEKRITERNRDP

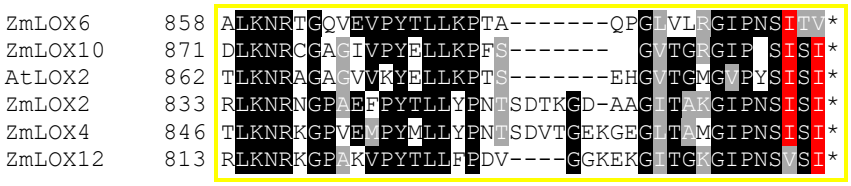

Figure 3-1. Multiple sequence alignment of *Zea mays* LOX6 gene with other plastid plant lipoxygenases and *Zea mays* 9-Lipoxygenases. Amino acid residues conserved in all proteins were shaded black and similar amino acids were shaded gray. Chloroplast transit peptides were boxed in with light green. The PLAT domain portion of the lipoxygenase was boxed in with light blue, and the Lipoxygenase domain of the lipoxygenase protein was boxed in with yellow. Highly conserved amino acid residues necessary for catalytic iron binding were shaded in red.

3.3.2 *mRNA transcript levels*

In order to characterize in vivo function of ZmLOX6, transgenic Arabidopsis plants using a ZmLOX6 overexpression cassette (Figure 2A) in wild type Col-0, and *rdr6-11* background. Hygromycin-resistant T_1 plants were identified and used to establish homozygous lines for in vivo analysis (Figure 2B). First, the expression level of ZmLOX6 mRNA in the transgenic lines were analyzed using RT-qPCR. Since ZmLOX6 is not present in untransformed control, ZmLOX6-OX transgenic line #68 was chosen as the reference line and the level of ZmLOX6 expression for each line was quantified relative to the line #68. Expression levels were 1.73, 1.22, 0.87 for lines 44, 72, and 70, respectively, showing approximately 2-fold variations among lines (Figure 1C). No LOX6 transcripts were detected in untransformed Col-0 or vector control plants.

3.3.3 *Flowering*

One obvious visible phenotype of ZmLOX6-OX plants was a change in flowering time. I measured flowering time of homozygous ZmLOX6-OX line (T_3

generation) along with control lines in two light regimens, long-day (16h light/8h dark) and day neutral (12h light /12h dark) conditions. Under both conditions ZmLOX6-OX lines flowered earlier. Using the long day conditions, flowering time in ZmLOX6-OX lines were reduced by 6.5, 5.6, 3.5, and 2.5 days for lines 44, 68, 70, and 72, respectively (Figure 2D) compared to untransformed Col-0. Interestingly, the number of resetting leaves and cauline leaves at the time of flowering were the same, suggesting early flowering phenotype was the result of rapid growth but not premature activation of flowering initiation.

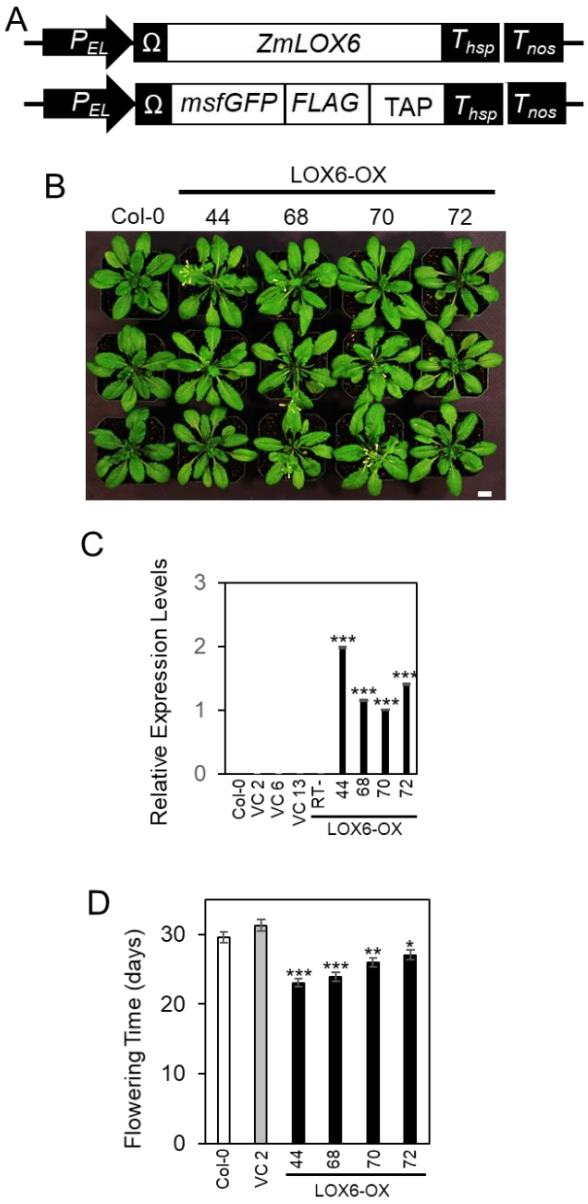

Figure 3-2. (A) Schematic representation of the expression Cassettes used in the analysis in this study. P_{EL}: CMV35S, **Ω**: (TMV**Ω**) Omega sequence, GFP : Green Fluorescence Protein, TAP: Tandem Affinity Purification, FLAG: 3x FLAG Tag, T_{nos}: Nos terminator sequence, T_{hsp}: Thermal heat shock protein terminator sequence. (B) Over expression of *Zea mays* LOX6 results in a mild to moderate chlorosis and early flowering. scale bar 1 cm. (C) Relative expression levels of ZmLOX6 overexpressed in stable T_3 *Arabidopsis thaliana* plants. (D) Days to flowering in stable transgenic ZmLOX6 Arabidopsis thaliana lines.

3.3.4 *Chlorophyll Analysis*

During the screening of ZmLOX6-OX T_1 seedlings, we found that the transformants became visibly chlorotic. Since chlorotic phenotype was previously linked with plant volatile productions (Napoli et al. 2014), we measured chlorophyll content of ZmLOX6-OX lines. We first analyzed the chlorophyll content of seedlings grown in vitro on 1/4 MS medium under sterilized conditions to ensure no biotic interactions occur between plant materials. Compared to untransformed control plants, ZmLOX6-OX lines showed significant decrease of chlorophyll content (24.1 %, 18 %, 17.7 %, and 18.2 % for lines 44, 68, 70, and 72, respectively, Figure 2A). Similar trends were observed for the plants grown on soil for 28-30 days (Figure 2B). No significant differences were observed between Col-0 and vector control lines. We then assessed to see if the volatiles from ZmLOX6-OX transgenic lines were able to impact plants in close proximity. In this experiment, untransformed Col-0 plants were placed adjacent to ZmLOX6-OX lines or isolated from ZmLOX6-OX lines. Interestingly, I found Col-0 plants adjacent to ZmLOX6-OX line 44 had 9.9% less chlorophyll content than Col-0 isolated (Figure 2C). *rdr6-11* adjacent to ZmLOX6-OX line 18 had 12% less chlorophyll content than *rdr6-11* isolated. These results indicated that overexpression of ZmLOX6 produced signals that could mimic ZmLOX6 overexpression in untransformed plants in close proximity.

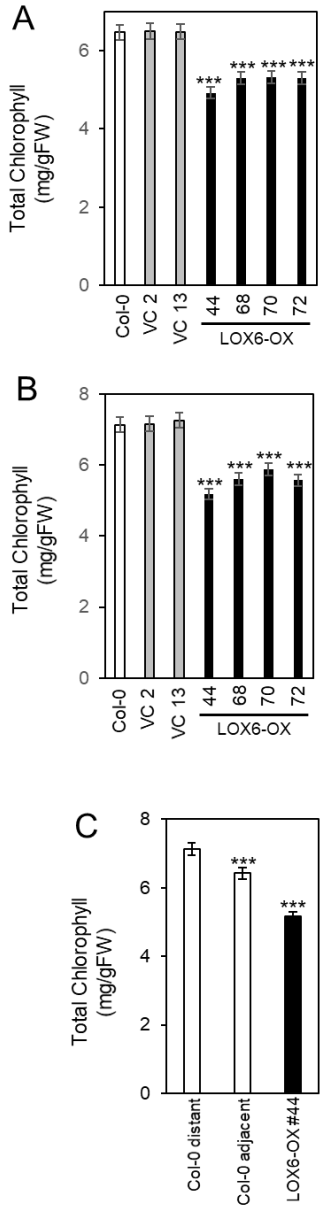

Figure 3-3. (A) Total chlorophyll content from 8-9 day old Arabidopsis plants grown on ¼ MS, 1.0% sucrose, 1.5% agar. 12mg of tissue was used in assessment. (B) Total chlorophyll content from 28-30 day old Arabidopsis plants grown on soil.10mg of tissue was used in assessment. (C) Total chlorophyll content for 28-30 day old soil grown untransformed Col-0 and *rdr6-11* in proximity of ZmLOX6-OX lines #44 and #18. 10mg of tissue were used in chlorophyll proximity experiments.

3.3.5 *Gas Chromatography Mass Spectrometry*

In order to test direct involvement of ZmLOX6 in production of volatile oxylipins in vivo, volatile profiles of ZmLOX6-OX plants were analyzed using GC-MS (Figure 4A). For comparison, Arabidopsis *lox2-1* mutant, which lacks nearly all volatile oxylipins (Mochizuki et al. 2016), was included. The GC/MS results revealed that ZmLOX6-OX lines produce much higher amounts of several C5 volatiles than untransformed Col-0, *rdr6-11*, vector control lines, and *Atlox2-1* mutant. ZmLOX6-enhanced C5 volatiles include C5 volatiles (E)-2-Pentenol, (E)-2-Pentenal, (Put) (Z)-2-Pentenal, 1-Penten-3-one, 3-Pentanone, and 3-Pentanol (Figure 4B). The levels of these C_5 volatiles are more consistent with ZmLOX6 transcript levels, with line 44 producing the highest amount for most of ZmLOX6-enhanced C5 volatiles. By contrast levels of C_6 volatiles are mostly unaffected by ZmLOX6 overexpression.

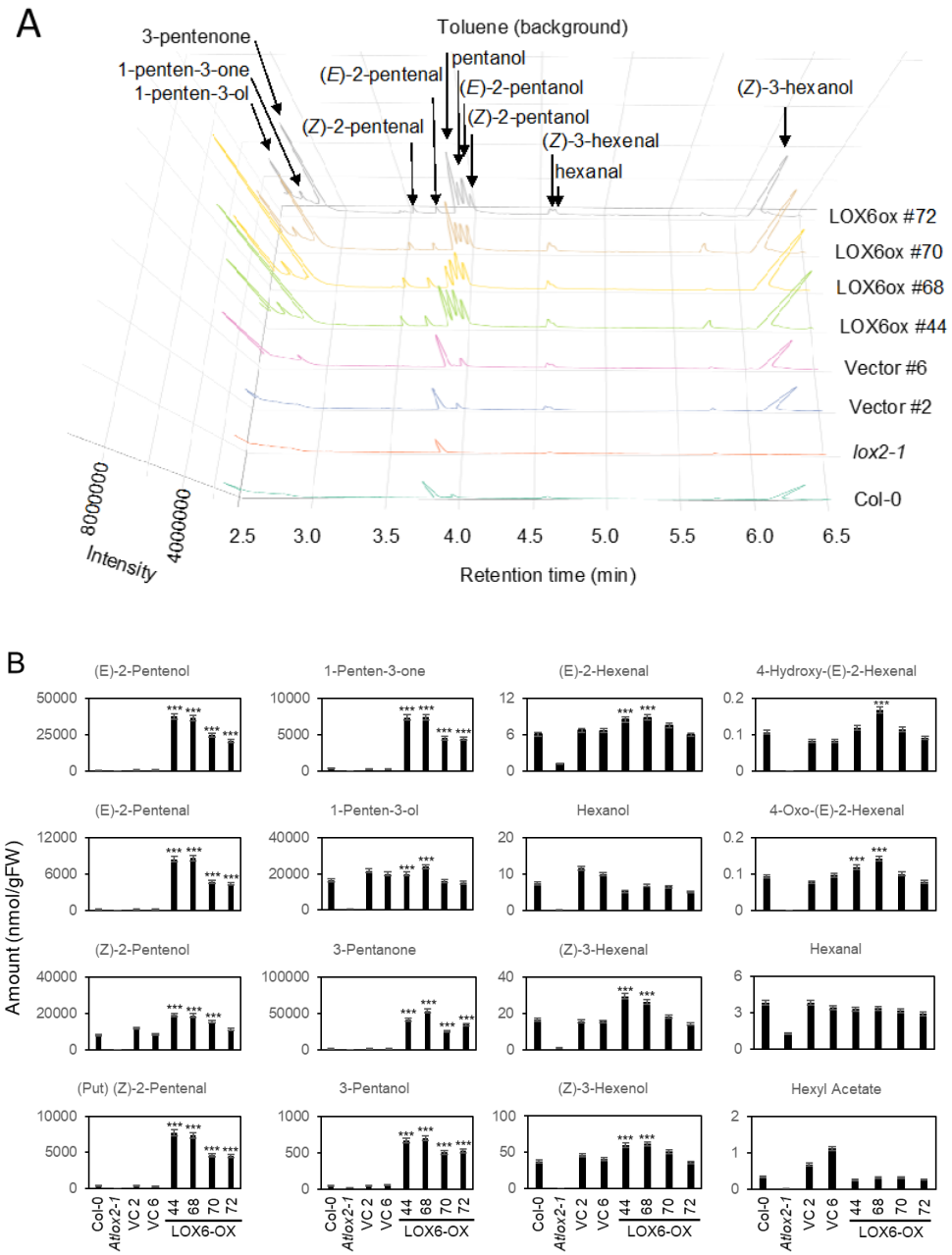

Figure 3-4. (A) Representative GC/MS chromatograms of C5 volatile compounds of cut up ZmLOX6 transgenic Arabidopsis leaves. (B) Amount of C_5 and C_6 volatile compounds in cut up ZmLOX6 transgenic Arabidopsis leaves. Mean values in ± SE (error bars) are shown (n = 5, technical replicates). Amounts of volatiles nmol/gFW

3.3.6 *Insect Choice Test*

Many plant volatiles serve as defensive compounds and promote resistance and deterrence to a variety of insect herbivory. The roles of plant oxylipin volatiles have been studied mainly with C_6 volatile known as green leafy volatiles (GLV) but little to no information regarding roles of C_5 volatiles and their impact on pathogen and insect behavior have been available. I took advantage of C5 volatile overproduction phenotype of ZmLOX6-OX plants and assessed the role of C_5 volatiles in plant-aphid interaction. I used choice test assay using green peach aphid, *Myzus persicae,* to see if there was any obvious difference in aphid preference to transgenic Arabidopsis ZmLOX6 lines over untransformed wild type (Figure 4). Starting with 30 aphids, line 44 and 72 had 7 and 3.7 more aphids per plant on average than Col-0. The result implied that aphids may recognize C_5 volatiles overproduced in ZmLOX6-OX as damage signals or weakness of plants and attracted by the volatiles.

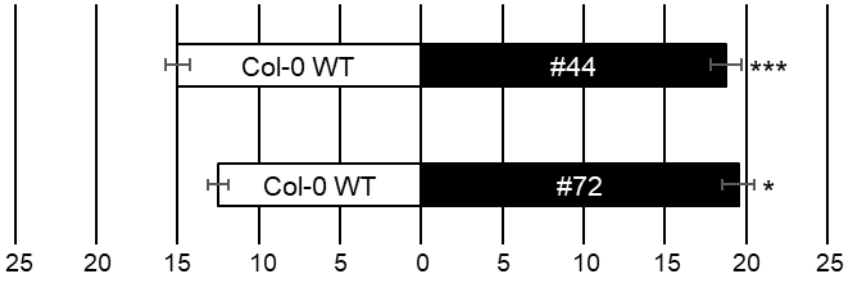

Figure 3-5. Three to Four week-old plants were used. The ZmLOX6-OX lines were larger by comparison to the untransformed Col-0 and *rdr6-11* plants. Settled aphids were counted at 24 hours after releasing. 30 aphids were released on the bridge between the two plants. Each test was comprised of 8 replicates, and three separate experiments.

3.4 Discussion Section

Plants have evolved a variety of chemical signaling pathways in order to survive in their ever-changing environments. As a result, unique means of communication that mediate local, systemic and plant to plant signaling were developed using various small molecule compounds. In this chapter, I characterized the unique features of ZmLOX6. Multiple sequence alignment analysis showed that many important amino acids of lipoxygenase proteins are conserved in ZmLOX6, while ZmLOX6 differs in key aspects that set it apart from all other LOX proteins, particularly in the C-terminal residue. I also examined the direct and indirect impacts of ZmLOX6 overexpression on plant growth and behavior. Analysis revealed that the overexpression of ZmLOX6 produced early flowering of the plants, but did not change the development of the plants. ZmLOX6 was also shown to alter the chlorophyll content of plants grown in vitro as well as soil grown plants, and untransformed plants in proximity to transgenic plants. The most prominent feature in ZmLOX6 overexpressing lines was the production of five-carbon volatiles. ZmLOX6 lines also showed a strong attraction to green peach aphids, which was opposite to the prediction that the aphids would be less attracted to plant defensive volatiles.

Biochemical analysis using bacterial recombinant protein of ZmLOX6 indicated that substrate of ZmLOX6 is lipid hydroperoxide (13-HPOT) generated by 13-LOX (Guo et al. 2008). In Arabidopsis, LOX2, a homolog of ZmLOX10, is responsible for production of various C_5 and C_6 volatiles (Mochizuki et al. 2016). Previous data (Christensen et al. 2013; Mochizuki et al. 2016) has shown that ZmLOX10/AtLOX2 is

responsible and essential for the formation of both GLVs and C_5 volatiles. The amounts of GLV's in intact leaf tissues were low, but upon disruption there is a large release (Mochizuki et al. 2016). By contrast there are large detectable amounts of C_5 volatiles that were detected in intact tissues, but upon wounding there was little change in their amounts. This all suggests that the biosynthetic pathways of GLVs and C_5 volatile compounds; which are both controlled by ZmLOX10/AtLOX2, but are differently regulated (Mochizuki et al. 2016).

The preliminary analysis of ZmLOX6 x *Atlox2-1* homozygous lines revealed moderate volatile production by comparison to *Atlox2-1* mutants. This suggests that ZmLOX6 may not be entirely dependent on ZmLOX10/AtLOX2 for substrate. Future analysis of ZmLOX6-OX crossed into Arabidopsis *lox2-1* mutant will address if ZmLOX6 is dependent on substrates produced by ZmLOX10/AtLOX2. Potential sources for volatile production from ZmLOX6 is first, ZmLOX6 is receiving substrate from some other source of plastid localizing lipoxygenase. This is possible considering 13-Lipoxygenases responsible for JA, not wound induced JA, such as ZmLOX8 or AtLOX3/AtLOX4 produce 13-LOX products (Christensen et al. 2013; Lunde et al. 2019; Acosta et al. 2009; Caldelari et al. 2011). That would however contradict known literature and evidence by both plant volatiles (Mochizuki et al. 2016). The second hypothesis is ZmLOX6 can produce its own substrate, acting both as a cleavage enzyme and a unique lipoxygenase enzyme. Based on the prediction by STRING v11 database (Price et al. 2016), ZmLOX6 may be able to complex with one or all of these lipases which can provide lipid substrate to ZmLOX6. This association may be the reason why

C_5 volatiles act differently than C_6 volatiles in disrupted tissues. As mentioned C_6 volatiles produce a “burst” of C_6 compounds from damaged tissues, while undamaged tissues maintain a low level of volatile release. On the contrary C_5 volatiles have a high level of constitutive emittion in undamaged tissues and only minimal to moderate increases in wounded tissues (Mochizuki et al. 2016). Immediate complexing of ZmLOX6 with chloroplast lipases may be a potential reason for the relatively high level of C_5 volatile presence even in uninduced plants.

CHAPTER IV

CONCLUSION

Chapter II establishes the subcellular localization of several maize 9-LOX and 9-LOX-like proteins, ZmLOX1, LOX4, LOX5, LOX6, LOX12, as well as OPR2 in stable transgenic Arabidopsis and maize protoplasts. Unlike near-exclusive plastid localization of 13-LOX, the localization patterns of 9-LOX proteins were diverse. They could be found in cytoplasm, plastids, tonoplasts, and unidentified protein body-like structure in the cytoplasm, which resembles aggresome. This establishment of the subcellular localization contributes to the overall understanding of 9-Lipoxygenase oxylipin biosynthesis in various cellular compartment. This chapter also took a look as to the overall protein domain functionality of LOX.

Chapter III characterizes the novel in vivo function of ZmLOX6 in production of C_5 volatiles, whose production and biological function are not well understood. Overexpression of ZmLOX6 increased the abundance of C_5 volatiles and caused moderate chlorosis, and promoted growth and flowering. Furthermore, I found ZmLOX6-OX plants were more attractive to aphids, perhaps due to the high levels of C_5 volatiles. At this point whether one or more of these volatiles, or the unique combination of these volatiles attract aphids is not clear.

In summary this thesis establishes the subcellular localization of most of the *Zea mays* 9-LOXs leaving the opportunity to understand further physiological and cellular function of 9-LOX isoforms. This thesis also provides the first assessment of *in vivo*

functionality of ZmLOX6-derived C_5 volatiles revealing their physiological impact on the host plant, and inter-plant and plant-herbivore communications.

REFERENCES

1. Acosta IF, Farmer EE. 2010. Jasmonates. Arabidopsis Book 8:e0129-e
2. Aksoy E, Jeong IS, Koiwa H. 2013. Loss of Function of Arabidopsis C-Terminal Domain Phosphatase-Like1 Activates Iron Deficiency Responses at the Transcriptional Level. Plant Physiology 161:330-45
3. Bang W, Kim S, Ueda A, Vikram M, Yun D, et al. 2006. Arabidopsis carboxyl-terminal domain phosphatase-like isoforms share common catalytic and interaction domains but have distinct in planta functions. Plant Physiol 142:586-94
4. Barton KA, Schattat MH, Jakob T, Hause G, Wilhelm C, et al. 2016. Epidermal Pavement Cells of Arabidopsis Have Chloroplasts. Plant Physiol 171:723-6
5. Bateman A, Sandford R. 1999. The PLAT domain: a new piece in the PKD1 puzzle. Curr Biol 9:R588-90
6. Betts MJ, Russell RB. 2003. Amino acid properties and consequences of substitutions. Bioinformatics for geneticists 317:289
7. Borrego EJ, Kolomiets MV. 2016. Synthesis and Functions of Jasmonates in Maize. Plants (Basel) 5
8. Bruce TJ, Pickett JA. 2011. Perception of plant volatile blends by herbivorous insects--finding the right mix. Phytochemistry 72:1605-11
9. Cacas J-L, Marmey P, Montillet J-L, Sayegh-Alhamdia M, Jalloul A, et al. 2008. A novel patatin-like protein from cotton plant, GhPat1, is co-expressed with

GhLox1 during Xanthomonas campestris-mediated hypersensitive cell death. Plant Cell Reports 28:155

10. Caldelari D, Wang G, Farmer EE, Dong X. 2011. Arabidopsis lox3 lox4 double mutants are male sterile and defective in global proliferative arrest. Plant Mol Biol 75:25-33

11. Canonne J, Froidure-Nicolas S, Rivas S. 2011. Phospholipases in action during plant defense signaling. Plant Signaling & Behavior 6:13-8

12. Chauvin A, Caldelari D, Wolfender JL, Farmer EE. 2013. Four 13-lipoxygenases contribute to rapid jasmonate synthesis in wounded Arabidopsis thaliana leaves: a role for lipoxygenase 6 in responses to long-distance wound signals. New Phytol 197:566-75

13. Chirala SS, Wakil SJ. 2004. Structure and function of animal fatty acid synthase. Lipids 39:1045-53

14. Christensen SA, Huffaker A, Kaplan F, Sims J, Ziemann S, et al. 2015. Maize death acids, 9-lipoxygenase–derived cyclopente(a)nones, display activity as cytotoxic phytoalexins and transcriptional mediators. Proceedings of the National Academy of Sciences 112:11407-12

15. Christensen SA, Nemchenko A, Borrego E, Murray I, Sobhy IS, et al. 2013. The maize lipoxygenase, ZmLOX10, mediates green leaf volatile, jasmonate and herbivore-induced plant volatile production for defense against insect attack. The Plant Journal 74:59-73

16. Christensen SA, Nemchenko A, Park Y-S, Borrego E, Huang P-C, et al. 2014. The Novel Monocot-Specific 9-Lipoxygenase ZmLOX12 Is Required to Mount an Effective Jasmonate-Mediated Defense Against Fusarium verticillioides in Maize. Molecular Plant-Microbe Interactions 27:1263-76

17. Clough SJ, Bent AF. 1998. Floral dip: a simplified method for Agrobacterium-mediated transformation of Arabidopsis thaliana. Plant J 16:735-43

18. Constantino N, Mastouri F, Damarwinasis R, Borrego E, Moran-Diez M, et al. 2013. Root-expressed maize lipoxygenase 3 negatively regulates induced systemic resistance to Colletotrichum graminicola in shoots. Front Plant Sci 4

19. Curtis MD, Grossniklaus U. 2003. A gateway cloning vector set for high-throughput functional analysis of genes in planta. Plant Physiol 133:462-9

20. Dai A. 2013. Increasing drought under global warming in observations and models. Nature Climate Change 3:52-8

21. De Moraes CM, Mescher MC, Tumlinson JH. 2001. Caterpillar-induced nocturnal plant volatiles repel conspecific females. Nature 410:577-80

22. Duan H, Huang M-Y, Palacio K, Schuler MA. 2005. Variations in CYP74B2 (Hydroperoxide Lyase) Gene Expression Differentially Affect Hexenal Signaling in the Columbia and Landsberg erecta Ecotypes of Arabidopsis. Plant Physiology 139:1529-44

23. Eek P, Piht M-A, Rätsep M, Freiberg A, Järving I, Samel N. 2015. A conserved π–cation and an electrostatic bridge are essential for 11R-lipoxygenase catalysis

and structural stability. Biochimica et Biophysica Acta (BBA) - Molecular and Cell Biology of Lipids 1851:1377-82

24. Egmond MR, Vliegenthart JFG, Boldingh J. 1972. Stereospecificity of the hydrogen abstraction at carbon atom n-8 in the oxygenation of linoleic acid by lipoxygenases from corn germs and soya beans. Biochemical and Biophysical Research Communications 48:1055-60

25. Ellinger D, Kubigsteltig II. 2010. Involvement of DAD1-like lipases in response to salt and osmotic stress in Arabidopsis thaliana. Plant Signaling & Behavior 5:1269-71

26. Ellinger D, Stingl N, Kubigsteltig II, Bals T, Juenger M, et al. 2010. DONGLE and DEFECTIVE IN ANTHER DEHISCENCE1 Lipases Are Not Essential for Wound- and Pathogen-Induced Jasmonate Biosynthesis: Redundant Lipases Contribute to Jasmonate Formation. Plant Physiology 153:114-27

27. Farmer EE, Ryan CA. 1990. Interplant communication: airborne methyl jasmonate induces synthesis of proteinase inhibitors in plant leaves. Proc Natl Acad Sci U S A 87:7713-6

28. Farmer EE, Ryan CA. 1992. Octadecanoid Precursors of Jasmonic Acid Activate the Synthesis of Wound-Inducible Proteinase Inhibitors. Plant Cell 4:129-34

29. Feussner I, Wasternack C. 2002. The lipoxygenase pathway. Annu Rev Plant Biol 53:275-97

30. Feys BJ, Wiermer M, Bhat RA, Moisan LJ, Medina-Escobar N, et al. 2005. Arabidopsis SENESCENCE-ASSOCIATED GENE101 Stabilizes

and Signals within an ENHANCED DISEASE SUSCEPTIBILITY1 Complex in Plant Innate Immunity. The Plant Cell 17:2601-13

31. Fischer AM, Dubbs WE, Baker RA, Fuller MA, Stephenson LC, Grimes HD. 1999. Protein dynamics, activity and cellular localization of soybean lipoxygenases indicate distinct functional roles for individual isoforms. Plant J 19:543-54

32. Fukudome A, Aksoy E, Wu X, Kumar K, Jeong IS, et al. 2014. Arabidopsis CPL4 is an essential C-terminal domain phosphatase that suppresses xenobiotic stress responses. Plant J 80:27-39

33. Gao X, Brodhagen M, Isakeit T, Brown SH, Gobel C, et al. 2009. Inactivation of the lipoxygenase ZmLOX3 increases susceptibility of maize to Aspergillus spp. Mol Plant Microbe Interact 22:222-31

34. Gao X, Stumpe M, Feussner I, Kolomiets M. 2008. A novel plastidial lipoxygenase of maize (Zea mays) ZmLOX6 encodes for a fatty acid hydroperoxide lyase and is uniquely regulated by phytohormones and pathogen infection. Planta 227:491-503

35. Golldack D, Li C, Mohan H, Probst N. 2014. Tolerance to drought and salt stress in plants: Unraveling the signaling networks. Front Plant Sci 5:151-

36. Hendriks T, Vreugdenhil D, Stiekema WJ. 1991. Patatin and four serine proteinase inhibitor genes are differentially expressed during potato tuber development. Plant Molecular Biology 17:385-94

37. Hou Q, Ufer G, Bartels D. 2016. Lipid signalling in plant responses to abiotic stress. Plant, Cell & Environment 39:1029-48

38. Hu X, Tanaka A, Tanaka R. 2013. Simple extraction methods that prevent the artifactual conversion of chlorophyll to chlorophyllide during pigment isolation from leaf samples. Plant Methods 9:19-

39. Hyun Y, Choi S, Hwang HJ, Yu J, Nam SJ, et al. 2008. Cooperation and functional diversification of two closely related galactolipase genes for jasmonate biosynthesis. Dev Cell 14:183-92

40. Ishiguro S, Kawai-Oda A, Ueda J, Nishida I, Okada K. 2001. The DEFECTIVE IN ANTHER DEHISCIENCE gene encodes a novel phospholipase A1 catalyzing the initial step of jasmonic acid biosynthesis, which synchronizes pollen maturation, anther dehiscence, and flower opening in Arabidopsis. Plant Cell 13:2191-209

41. Jeong IS, Fukudome A, Aksoy E, Bang WY, Kim S, et al. 2013. Regulation of abiotic stress signalling by Arabidopsis C-terminal domain phosphatase-like 1 requires interaction with a k-homology domain-containing protein. PLoS One 8:e80509

42. Koiwa H, Bressan RA, Hasegawa PM. 1997. Regulation of protease inhibitors and plant defense. Trends in Plant Science 2:379-84

43. Kong JM, Chia LS, Goh NK, Chia TF, Brouillard R. 2003. Analysis and biological activities of anthocyanins. Phytochemistry 64:923-33

44. Kuhn H, Belkner J, Wiesner R, Brash AR. 1990. Oxygenation of biological membranes by the pure reticulocyte lipoxygenase. J Biol Chem 265:18351-61

45. Lim GH, Singhal R, Kachroo A, Kachroo P. 2017. Fatty Acid- and Lipid-Mediated Signaling in Plant Defense. Annu Rev Phytopathol 55:505-36

46. Lloyd-Price J, Abu-Ali G, Huttenhower C. 2016. The healthy human microbiome. Genome Medicine 8:51

47. Lunde C, Kimberlin A, Leiboff S, Koo AJ, Hake S. 2019. Tasselseed5 overexpresses a wound-inducible enzyme, ZmCYP94B1, that affects jasmonate catabolism, sex determination, and plant architecture in maize. Communications Biology 2:114

48. Matsui K, Irie M, Kajiwara T, Hatanaka A. 1992. Developmental changes in lipoxygenase activity in cotyledons of cucumber seedlings. Plant Science 85:23-32

49. Matsui K, Sugimoto K, Mano Ji, Ozawa R, Takabayashi J. 2012. Differential Metabolisms of Green Leaf Volatiles in Injured and Intact Parts of a Wounded Leaf Meet Distinct Ecophysiological Requirements. PLOS ONE 7:e36433

50. Mochizuki S, Sugimoto K, Koeduka T, Matsui K. 2016. Arabidopsis lipoxygenase 2 is essential for formation of green leaf volatiles and five-carbon volatiles. FEBS Letters 590:1017-27

51. Mueller MJ, Berger S. 2009. Reactive electrophilic oxylipins: Pattern recognition and signalling. Phytochemistry 70:1511-21

52. Nakamura S, Hatanaka A. 2002. Green-leaf-derived C6-aroma compounds with potent antibacterial action that act on both Gram-negative and Gram-positive bacteria. J Agric Food Chem 50:7639-44

53. Nalam VJ, Keeretaweep J, Sarowar S, Shah J. 2012. Root-derived oxylipins promote green peach aphid performance on Arabidopsis foliage. Plant Cell 24:1643-53

54. Neitzel J. 2010. Positive Behavior Supports for Children and Youth with Autism Spectrum Disorders. Preventing School Failure: Alternative Education for Children and Youth 54:247-55

55. Ni M, Cui D, Einstein J, Narasimhulu S, Vergara CE, Gelvin SB. 1995. Strength and tissue specificity of chimeric promoters derived from the octopine and mannopine synthase genes. The Plant Journal 7:661-76

56. Ohlrogge J, Browse J. 1995. Lipid biosynthesis. Plant Cell 7:957-70

57. Okazaki Y, Saito K. 2014. Roles of lipids as signaling molecules and mitigators during stress response in plants. Plant J 79:584-96

58. Park YS, Kunze S, Ni X, Feussner I, Kolomiets MV. 2010. Comparative molecular and biochemical characterization of segmentally duplicated 9-lipoxygenase genes ZmLOX4 and ZmLOX5 of maize. Planta 231:1425-37

59. Rips S, Bentley N, Jeong IS, Welch JL, von Schaewen A, Koiwa H. 2014. Multiple N-glycans cooperate in the subcellular targeting and functioning of Arabidopsis KORRIGAN1. Plant Cell 26:3792-808

60. Robert S, Zouhar J, Carter C, Raikhel N. 2007. Isolation of intact vacuoles from Arabidopsis rosette leaf-derived protoplasts. Nat Protoc 2:259-62

61. Scala A, Allmann S, Mirabella R, Haring MA, Schuurink RC. 2013. Green leaf volatiles: a plant's multifunctional weapon against herbivores and pathogens. Int J Mol Sci 14:17781-811

62. Schaller F. 2001. Enzymes of the biosynthesis of octadecanoid‐derived signalling molecules. Journal of Experimental Botany 52:11-23

63. Segami S, Makino S, Miyake A, Asaoka M, Maeshima M. 2014. Dynamics of Vacuoles and H⁺-Pyrophosphatase Visualized by Monomeric Green Fluorescent Protein in Arabidopsis: Artifactual Bulbs and Native Intravacuolar Spherical Structures. The Plant Cell 26:3416-34

64. Senda K, Yoshioka H, Doke N, Kawakita K. 1996. A cytosolic phospholipase A2 from potato tissues appears to be patatin. Plant Cell Physiol 37:347-53

65. Sofo A, Dichio B, Xiloyannis C, Masia A. 2004. Lipoxygenase activity and proline accumulation in leaves and roots of olive trees in response to drought stress. Physiologia Plantarum 121:58-65

66. Song WC, Funk CD, Brash AR. 1993. Molecular cloning of an allene oxide synthase: a cytochrome P450 specialized for the metabolism of fatty acid hydroperoxides. Proc Natl Acad Sci U S A 90:8519-23

67. Staswick PE, Tiryaki I. 2004. The oxylipin signal jasmonic acid is activated by an enzyme that conjugates it to isoleucine in Arabidopsis. Plant Cell 16:2117-27

68. Tamogami S, Rakwal R, Agrawal GK. 2008. Interplant communication: Airborne methyl jasmonate is essentially converted into JA and JA-Ile activating jasmonate signaling pathway and VOCs emission. Biochemical and Biophysical Research Communications 376:723-7

69. Tolley JP, Nagashima Y, Gorman Z, Kolomiets MV, Koiwa H. 2018. Isoform-specific subcellular localization of Zea mays lipoxygenases and oxo-phytodienoate reductase 2. Plant Gene 13:36-41

70. Tranbarger TJ, Franceschi VR, Hildebrand DF, Grimes HD. 1991. The soybean 94-kilodalton vegetative storage protein is a lipoxygenase that is localized in paraveinal mesophyll cell vacuoles. Plant Cell 3:973-87

71. van Den Dool H, Dec. Kratz P. 1963. A generalization of the retention index system including linear temperature programmed gas—liquid partition chromatography. Journal of Chromatography A 11:463-71

72. van den Ingh TSGAM, Krogdahl Å, Olli JJ, Hendriks HGCJM, Koninkx JGJF. 1991. Effects of soybean-containing diets on the proximal and distal intestine in Atlantic salmon (Salmo salar): a morphological study. Aquaculture 94:297-305

73. Vandendool H, Kratz PD. 1963. A GENERALIZATION OF THE RETENTION INDEX SYSTEM INCLUDING LINEAR TEMPERATURE PROGRAMMED GAS-LIQUID PARTITION CHROMATOGRAPHY. J Chromatogr 11:463-71

74. Vellosillo T, Aguilera V, Marcos R, Bartsch M, Vicente J, et al. 2013. Defense activated by 9-lipoxygenase-derived oxylipins requires specific mitochondrial proteins. Plant Physiol 161:617-27

75. Vernooy-Gerritsen M, Leunissen JL, Veldink GA, Vliegenthart JF. 1984. Intracellular localization of lipoxygenases-1 and -2 in germinating soybean seeds by indirect labeling with protein a-colloidal gold complexes. Plant Physiol 76:1070-8

76. Vickers CE, Gershenzon J, Lerdau MT, Loreto F. 2009. A unified mechanism of action for volatile isoprenoids in plant abiotic stress. Nat Chem Biol 5:283-91

77. Vishwanath VA. 2016. Fatty Acid Beta-Oxidation Disorders: A Brief Review. Ann Neurosci 23:51-5

78. Wang YS, Yang ZM. 2005. Nitric oxide reduces aluminum toxicity by preventing oxidative stress in the roots of Cassia tora L. Plant Cell Physiol 46:1915-23

79. War AR, Sharma HC, Paulraj MG, War MY, Ignacimuthu S. 2011. Herbivore induced plant volatiles: their role in plant defense for pest management. Plant Signal Behav 6:1973-8

80. Wardale DA, Ambert EA. 1980. Lipoxygenase from cucumber fruit: Localization and properties. Phytochemistry 19:1013-6

81. Wasternack C, Strnad M. 2016. Jasmonate signaling in plant stress responses and development - active and inactive compounds. N Biotechnol 33:604-13

82. Wei J, Wang L, Zhu J, Zhang S, Nandi OI, Kang L. 2007. Plants attract parasitic wasps to defend themselves against insect pests by releasing hexenol. PLoS One 2:e852

83. Xu Y, Ishida H, Reisen D, Hanson MR. 2006. Upregulation of a tonoplast-localized cytochrome P450 during petal senescence in Petunia inflata. BMC Plant Biology 6:8

84. Xue YJ, Tao L, Yang ZM. 2008. Aluminum-induced cell wall peroxidase activity and lignin synthesis are differentially regulated by jasmonate and nitric oxide. J Agric Food Chem 56:9676-84

85. Yamauchi Y, Kunishima M, Mizutani M, Sugimoto Y. 2015. Reactive short-chain leaf volatiles act as powerful inducers of abiotic stress-related gene expression. Scientific Reports 5:8030

86. Zaarur N, Meriin AB, Gabai VL, Sherman MY. 2008. Triggering aggresome formation. Dissecting aggresome-targeting and aggregation signals in synphilin 1. J Biol Chem 283:27575-84

87. Zhang J, Simmons C, Yalpani N, Crane V, Wilkinson H, Kolomiets M. 2005. Genomic analysis of the 12-oxo-phytodienoic acid reductase gene family of Zea mays. Plant Mol Biol 59:323-43

88. Zhang Y, Werling U, Edelmann W. 2012. SLiCE: a novel bacterial cell extract-based DNA cloning method. Nucleic Acids Res 40:e55

APPENDIX A

Table 1-1. Primer sequences used for thesis project

Primer	Name	Sequence
922	GFPF	ATGAGCAAGGGCGAGGAGCT
923	GFPR	tta<TTTGTACAGCTCGTCCATGC
1444	SLiCELOX2F	ATTTACAATTACAGTCGAccatgTTCGGAAACATCGGAAAG
1445	SLiCELOX2R	TCCTCGCCCTTGCTCACCTCGAGTCCACCGCCACC<GATGGAAATGCTGTTGGGGA
1428	SLICELOX4/5F	TTACTATTTACAATTACAGTCGACCATGTTCTGGCACGGGGTCGC
1429	SLICELOX4/5R	ACAGCTCCTCGCCCTTGCTCACCTCGAGTCCACCGCCACCTATGGAGATGCTGTTGGGAA
1430	SLICELOX6F	TTACTATTTACAATTACAGTCGACCATGATGCAGCAGCTCCGT
1431	SLICELOX6R	ACAGCTCCTCGCCCTTGCTCACCTCGAGTCCACCGCCACCAACGGTGATGCTGTTGGGTA
1434	mCherry2-G4-LOX6NR	TCCTCGCCCTTGCTCACCATGCCACCGCCACCGACATGCACGCTCGTAGGCG
1435	mCherry2F	ATGGTGAGCAAGGGCGAGGA
1436	mCherry2R	CTTGTACAGCTCGTCCATGC
1437	mCherry2-G4-LOX6CF	CACCGGCGGCATGGACGAGCTGTACAAGGGTGGTGGCGGTAAGCTGCTGCTGCAGAACTT
1438	Nos-LOX6R	GCCAAATGTTTGAACGATCGGGGAAATTCGAGCTCTCAAACGGTGATGCTGTTGG
T1	SLiCE LOX12F	TTACTATTTACAATTACAGTCGACCATGCAAATGCCCTCTGTCC
T2	SLiCE LOX12R	ACAGCTCCTCGCCCTTGCTCACCTCGAGTCCCACCGCCACCTATGGAGACGCTGTTGGGTA
1432	SLICEOPR2F	TTACTATTTACAATTACAGTCGACCATGGTGCAGCAAGCCGCGAAGGA
1433	SLICEOPR2R	ACAGCTCCTCGCCCTTGCTCACCTCGAGTCCACCGCCACCCTCCTCATTCTTGCCATCTT
T32	LOX4Δ9F	ggaaaaCGGACCGcaatctctactcccaggaacgcg
T33	LOX4Δ9R	tggggattctcttcctgacctct
T34	LOX4Δ11F	ggaaaaCGGACCGcgtacacaggatcctcggct
T35	LOX4Δ11R	gtgcgggtagatccacgagtt
1159	IntseqF	ATCGGTTTGAATCCGATAGC
1454	LOX6screenF1	AAGTACCGGGAGGACGAGGT
1455	LOX6screenF2	TGAAGCGCATCAACGAGCTC

T51	LOX6screenF3	GAAAACTGCAACCGAGCGTC
T23	LOX6F-Blunt	ATGCAGCAGCTCCCGTCACAG
T24	LOX6R-NotI	GGAAAAGCGGCCGCTTAAACGGTGATGCTGTTGGGTATG
T45	LOX6-qPCR Set 1 F	CTCTTCCCAACGATCTCATCAA
T46	LOX6-qPCR Set 1 R	GCGTACGGGTAGTCCTTTATC
T47	LOX6-qPCR Set 5 F	CAAGGACCATGTCGAGAAGAA
T48	LOX6-qPCR Set 5 R	GTTGATGCGCTTCAGGTATG
T49	Atlox2-1 F	GGATTATCATGATTTGCTTCTACC
T50	Atlox2-1 R	TCAAATAGAAATACTATAAGGAACAC